



Chironomid assemblages in surface sediments from 182 lakes across New England and Eastern Canada: Development and validation of a new summer temperature transfer function

Thomas Suranyi^{a,b,*}, Julie Talbot^a, Donna Francis^c, Augustin Feussom Tcheumeleu^{a,b}, Pierre Grondin^d, Damien Rius^b, Adam A. Ali^{e,f,g}, Yves Bergeron^{f,g}, Laurent Millet^b

^a Département de Géographie, Université de Montréal, Campus MIL, 1375 Avenue Thérèse Lavoie-Roux, Montréal, Québec, H2V 0B3, Canada

^b Laboratoire Chrono-environnement, UMR 6249, CNRS, Université Franche-Comté, 16 route de Gray, 25030, Besançon cedex, France

^c Department of Earth, Geographic, and Climate Sciences, University of Massachusetts, Amherst, MA, USA

^d Ministère des Forêts, de la Faune et des Parcs, Direction de la recherche forestière, Québec, Canada

^e Institut des Sciences de l'Évolution, UMR 5554, CNRS-IRD-Université Montpellier-EPHE, Montpellier, France

^f Centre d'étude de la Forêt, Université du Québec à Montréal, Montréal, Québec, Canada

^g Institut de recherche sur les forêts, Université du Québec en Abitibi-Témiscamingue, Rouyn-Noranda, Québec, Canada

1. Introduction

Reconstructing natural climate variability is fundamental to understanding past ecosystem dynamics (van Bellen et al., 2011; Blarquez et al., 2015; Girardin et al., 2024; Magnan et al., 2019). Subfossil chironomid assemblages can serve as indicators of past summer temperatures in such investigations. Due to their relative independence from terrestrial vegetation, they provide a valuable complement to pollen-based paleoclimatic reconstructions, which may be susceptible to circular reasoning when examining climate-vegetation relationships (Birks et al., 2010).

Chironomidae (Diptera) larvae are both abundant and highly diverse in lake ecosystems. Each larval instar produces a chitinous cephalic capsule that preserves well in sediments and can be identified to genus or species morphotype (Brooks et al., 2007). Across the Holarctic, modern chironomid taxa in lake surface sediments are primarily influenced by summer air and surface water temperatures (Fortin et al., 2015; Heiri et al., 2011; Walker et al., 1997). This modern chironomid-temperature relationship enables the development of quantitative inference models that can be applied to downcore subfossil assemblages to produce paleotemperature estimates. Overall, chironomid-inferred summer temperature reconstructions align well with other proxies and meteorological measurements (Holmes et al., 2011; Larocque et al., 2009; Luoto et al., 2019; Luoto and Ojala, 2017; Self et al., 2011). However, the chironomid-temperature relationship is complex and involves multiple direct and indirect influences

(Eggermont and Heiri, 2012). This complexity can introduce uncertainties and potential biases in temperature reconstructions due to confounding environmental factors, such as lake depth and water pH (Mayfield et al., 2024; Velle et al., 2010). Even if the usefulness of subfossil chironomids in paleoclimatology is well established (Brooks et al., 2012), the application of transfer functions requires careful ecological interpretation to assess the drivers of downcore assemblage changes and ensure reliable reconstructions (Hohmann et al., 2023; Juggins, 2013; McKeown et al., 2019; Velle et al., 2012). A deep understanding of the ecological and statistical foundations of the chironomid-temperature relationship is therefore crucial to fully leverage the insights of transfer function-based paleotemperature reconstructions.

In Quebec, Larocque et al. (2006) and Larocque (2008) developed a chironomid-temperature transfer function using a calibration dataset with high taxonomic resolution, which was successfully applied to reconstruct summer temperature in the eastern Canadian boreal forest (Bajolle et al., 2018; Feussom Tcheumeleu et al., 2023). However, this transfer function only includes a few lakes south of the Quebec logging limit (Fig. 1), limiting its applicability to lower latitudes. Extending its application further south would likely introduce an underestimation bias due to the edge-effect (Birks, 1995).

Another concern arises from the numerical technique used to develop the temperature inference model. The widely used weighted average partial least square model (WAPLS; ter Braak and Juggins, 1993) has remained largely unchanged for over two decades. This

This article is part of a special issue entitled: Holocene in the sub-Arctic published in Quaternary Science Reviews.

* Corresponding author. Département de Géographie, Université de Montréal, Campus MIL, 1375 Avenue Thérèse Lavoie-Roux, Montréal, Québec, H2V 0B3, Canada.

E-mail address: thomas.suranyi@umontreal.ca (T. Suranyi).

<https://doi.org/10.1016/j.quascirev.2025.109333>

Received 16 July 2024; Received in revised form 24 February 2025; Accepted 26 March 2025

Available online 5 April 2025

0277-3791/© 2025 The Authors. Published by Elsevier Ltd. This is an open access article under the CC BY-NC license (<http://creativecommons.org/licenses/by-nc/4.0/>).

method estimates taxon optima for the variable of interest under the assumption of unimodal responses and then use the residual structure to improve the fit of the model (Birks, 1995). However, it does not account for differences in tolerance among taxa, meaning that valuable ecological information embedded in taxon distributions remains underutilized for inference. Furthermore, WAPLS does not make any correction for unequal sampling designs, where some climatic values are over-represented in the calibration dataset. This imbalance can lead to biases in estimates from WAPLS (Liu et al., 2020). To address these issues Liu et al. (2020) developed an improved version of WAPLS, the frequency-corrected tolerance-weighted WAPLS (fxTWAPLS). This method accounts for sampling biases and taxon-specific tolerances, demonstrating improved performance in pollen-based climate reconstructions through both cross-validation and downcore applications. This promising method has not yet, to our knowledge, been applied to other paleoclimatic proxies and its potential for chironomid-based summer temperature reconstructions remains unexplored.

Our goal is to develop a versatile Chironomidae-based transfer function by integrating existing datasets with newly sampled lakes across a wide latitudinal gradient, to enhance the spatial and ecological coverage necessary for robust paleotemperature reconstructions. This transfer function will provide a reliable pollen-independent approach for reconstructing Holocene summer temperature changes within a multi-proxy framework, facilitating the study of climate change impacts on ecosystems and human activities in the northeastern Nearctic.

To achieve this, we define three specific objectives.

- (1) Investigate the climatic and limnological drivers of taxonomic composition in subfossil Chironomidae assemblages using a newly developed calibration dataset spanning a broad latitudinal gradient, from temperate to Arctic regions. We expect summer temperature to be the dominant driver, which is a prerequisite for transfer function development.

- (2) Evaluate summer temperature inference models by comparing the widely used WAPLS with the newly developed fxTWAPLS technique. Performance assessment involves cross-validation and comparison of downcore temperature reconstructions with weather station data from two contrasting Nearctic bioclimatic settings: the Laurentian Mountains (southern Quebec; Lake Croche) and southwestern Greenland (Lake Igaliku).
- (3) Assess the improvements introduced by the new transfer function by applying it to a previously published 8500-year subfossil record from the eastern Canadian boreal forest (Lake Mista). This will refine postglacial summer temperature reconstruction at this site and further evaluate the robustness of the fxTWAPLS approach for chironomid-based paleoclimatic studies.

2. Materials and methods

2.1. Lake surface sediment calibration dataset

The modern distribution of Chironomidae taxa was assessed based on the analysis of subfossil head capsules from surface sediments from 182 lakes located in eastern Canada and northeastern United States. These lakes were aggregated from three previously published datasets of New England (36 sites; Francis, 2004), northwestern Quebec (61 sites; Larocque, 2008; Larocque et al., 2006; available online since Bajolle et al., 2018) and Baffin Island (26 sites; Francis et al., 2006) along with 59 new sites from southern Quebec and Labrador region sampled between 2019 and 2022 (Fig. 1; Table 1). For the northwestern Quebec dataset Lakes A to J had no geographical coordinates available and therefore have not been included in the final calibration dataset of this paper. The three published datasets were chosen to cover a maximal climatic range within each respective region. The 59 new lakes were therefore sampled primarily in southern Quebec with the same objective in mind, to obtain a calibration dataset with a near continuous

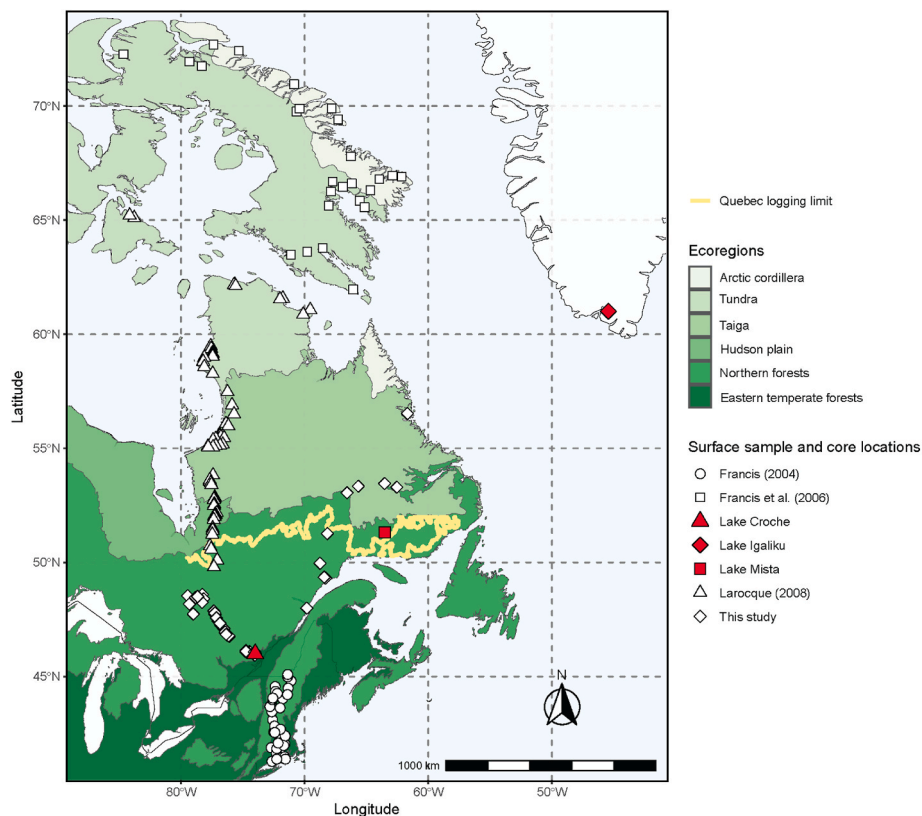


Fig. 1. Sampling location of the 182 modern chironomid assemblages included in the transfer function and the three studied fossil records (Lakes Igaliku, Mista and Croche). North American ecoregions are outlined to show the climatic gradient covered by the training-set (U.S. Environmental Protection Agency, 2016).

Table 1

Summary of the characteristics of the four data subsets used to create the calibration dataset of this paper.

Dataset	N (number of lake)	Latitude (°N)	Longitude (°W)	JJA (°C)	Depth (m)	pH	Conductivity (µS/cm)
Francis et al. (2006)	26	61.96–72.70	84.68–62.17	0.3–6.97	3.6–43.80	4.66–7.36	1.21–30.11
Larocque (2008)	61	49.8–65.21	84.17–69.55	6.03–14.87	1.0–36.5	5.1–7.60	1.6–230.0
Francis (2004)	36	41.31–45.10	72.82–71.11	16.1–21.20	1.02–13.30	4.62–8.30	9.5–114.2
New sites	59	45.92–56.52	79.47–61.70	9.43–17.63	1.1–31.0	4.62–8.30	1.6–220.6
Total	182	41.31–72.70	84.68–61.70	0.3–21.2	1.0–43.80	4.62–8.30	1.21–230.0

latitudinal gradient spanning the full range of the Quebec province and covering more than 20 °C of mean summer air temperature.

We refer readers to the original publications for information on the sampling methods of sites used in the previously published datasets. For the 59 new sites of Quebec-Labrador, we collected the first centimetre of sediment at the deepest point of each lake with an interface Uwitec corer. We measured physico-chemical profiles in the water column using a YSI EXO3 multiparameter sonde (water temperature, depth, pH, conductivity, dissolved oxygen), and collected a sample of water 50 cm below the lake surface, later analysed at the GRIL laboratory for dissolved organic carbon, total phosphorus, and total nitrogen concentrations on both filtered and non-filtered water. We extracted chironomid head capsules (HC) from surface sediments according to the standard treatment procedure i.e., bath of KOH (10 %) before being sieved at 100 µm and hand-sorting of sieved residue under 40 to 70 × magnification. Then, we prepared microscope slides of HC using Aquatex® mounting agent. Identifications were performed to genus or morphotype-level following (Brooks et al., 2007; Epler, 2001; Oliver and Roussel, 1983; Wiederholm, 1983) under 100 to 1000 × magnification. For ensuring a better reproducibility with a consistent taxonomic harmonization without the opportunity to cross-check slides between previously established training-sets, we had to merge some related morphotypes. *Psectrocladius calcaratus*-type and *P. septentrionalis*-type were merged in *Monopsectrocladius*, and *Heterotrissocladius subpilosus*-type was merged with *H. maeeri*-type 1 and type 2 because of possible inconsistent identification between analysts. Those changes had only minor influences on the inference models and subsequent reconstructions, but we opted for a conservative approach. We calculated the percentage of each taxon to the total number of HC in each sample. For the final dataset we kept only taxa occurring in at least two lakes and with a maximum of relative abundance reaching at least 2 %. We compared chironomid abundances to three limnological variables, namely lake depth, pH and conductivity because they are the only limnological variables available for almost all lakes of the calibration dataset, in addition to mean June–July–August air temperature (hereafter, JJA temperatures) derived from Worldclim 2.1 gridded climatic data at 30 s resolution (Fick and Hijmans, 2017). The Worldclim 2.1 dataset provided uniform average monthly mean air temperatures for the 1970–2000 CE period on all sites despite the scarcity of meteorological records across the study area.

We acknowledge that certain variables not directly included in our analysis, such as nutrients, dissolved oxygen (DO), and dissolved organic carbon (DOC), play an important role in shaping chironomid assemblages (Brodersen et al. 2002; Luoto et al., 2016; Quinlan and Smol, 2001). While these factors could have provided additional insight, they often covary with climate (Dranga et al., 2018; Larocque et al., 2006) and are themselves involved in temperature-driven lake processes. Consequently, their influence is indirectly captured in our analysis of the chironomid-temperature relationship, which inherently reflects temperature-mediated changes in lake characteristics (Eggermont and Heiri, 2012). Given our focus on temperature reconstruction, this potential limitation does not preclude the achievement of our objectives.

2.2. Downcore subfossil records

We tested the ability of the new transfer function to reconstruct an

already established climatic signal from subfossil chironomid data in Arctic conditions using data from Lake Igaliku (61°00' N, 45°26' W; 15 m asl; max depth Zmax 26 m; southern Greenland; Fig. 1), where Millet et al. (2014) demonstrated that changes in the chironomid fauna (PCA 1 scores) were significantly correlated with JJA temperatures during part of the instrumental period (1879–1988 CE). We used chironomid data from the sediment samples ranging from 1879 to 1988 CE and compared chironomid-inferred temperatures to JJA temperatures measured at Ivittuut weather station (1873–1960 CE) and Narsarsuaq Weather station (1961–1988 CE) after calculation of the mean value for the years covered by each sample.

Lake Croche (45°59' N, 74°00' W; 359 m asl; southern Quebec; Fig. 1) is a 17.9 ha multi-depression lake composed of three mains basin with similar maximum depths (Zmax 11.4 m). It is located within the Laurentian Biological Station of the University of Montreal and has a predominantly forested watershed that has been protected from anthropogenic activities (except for research) since the 1960s. Mean annual temperature measured from the nearest weather station (1.05 km away of the lake; St-Hippolyte station; 45°59' N, 74°00' W; 366 m asl) is 4.3 °C, and JJA average temperature is 17.8 °C for the 1981–2010 period. In June 2021, a sediment core was retrieved from the deepest part (10 m) of the central basin of the lake with a UWITEC gravity corer. We sliced the top 17 cm of the core at 0.5 cm intervals and the remainder at 1 cm intervals. The core chronology was established using thirty-eight α-spectrometry ²¹⁰Pb measurements (top 20 cm of the core) processed with a constant rate of supply model (Appleby and Oldfield, 1978; Supplemental Fig. S1). Subfossil chironomid analysis was performed as described in section 2.1 on the first fifteen samples at 1 cm interval on the core. The meteorological data used for the reconstruction performance assessment comes from the weather stations of St-Hippolyte (1964–2017 CE) and St-Jerome (45°48' N, 74°03' W; 170 m asl; 1932–1963 CE). The data from St-Jerome (~20 km away of the Lake Croche) were corrected for lower latitude and altitude by a linear model with data from St-Hippolyte based on the 1964–2017 CE period (p-value < 0.001; adjusted R² = 0.87; RMSE = 0.31 °C; Supplemental Fig. S2).

Lake Mista (51°06' N, 63°26' W; 500 m asl; Fig. 1) is a small head-water lake with a maximum water depth of 5 m, located in the eastern coniferous boreal forest of Quebec. The subfossil chironomid data are from Feussom Tcheumeleu et al. (2023) who described postglacial (roughly the last 8500 years) changes in the chironomid fauna based on 79 samples from a 373-cm core. We established a Bayesian age-depth model for the core using RBAACON R package (Blaauw and Christen, 2011; Supplemental Fig. S3) from radiocarbon dates indicated in the original publication of the Lake Mista record.

2.3. Numerical analysis

All numerical analyses were performed using R v4.2.2 (R Core Team, 2022). We used several data analyses inspired from the reference guide of Borcard et al., (2018) to constrain the response of chironomids by environmental explanatory data. We performed a multivariate regression tree (MRT (De'ath, 2002; Larsen and Speckman, 2004)); using the function *mypart()* of the *MVPART* package (De'ath 2007) corrected locally and working on later versions of R software (available upon request). This method can directly assess non-linear effects and interactions

between explanatory variables. We also combined the MRT partition of sites with an indicator taxa analysis using the IndVal index (Dufrene and Legendre, 1997) and the *multipatt()* function from `INDICESPECIES` package (Cáceres and Legendre, 2009), allowing for the identification of indicator taxa for each group of the MRT partition but also for different combinations of groups. We assessed statistical significance (p -value < 0.05) of the indicative value of each taxon using a corrected p -value for multiple tests with *p.adjust()* from the `STATS` package. Hellinger transformation-based redundancy analysis (tb-RDA) and resulting ordination triplots were produced to find gradients into the structure of chironomid data that could be explained by environmental variables. We used the *rda()* function of the `VEGAN` package (Oksanen et al., 2023) and determined the part of variance explained by our constraints with an adjusted R^2 (Peres-Neto et al., 2006) thanks to the *RsquareAdj()* function. The statistical significance of the tb-RDA and of each canonical axes was assessed by permutation tests (999) to determine if the amount of the represented variation differs significantly from a random distribution (Legendre et al., 2011). We also produced a Venn diagram resulting from variation partitioning implying a set of different partial tb-RDA (Borcard et al., 1992; Peres-Neto et al., 2006) to illustrate quantitatively the different parts of the total variance explained by each constraint alone or shared between them. The *varpart()* function of `VEGAN` was used for this purpose. We applied the Hellinger transformation on chironomid data for the MRT and the RDAs (including those of the variation partitioning) because these methods rely on the calculation of Euclidean distances between objects, which is not directly adapted for ecological community datasets (Legendre and Legendre, 2012). This transformation alters the geometry of the data prior to analysis, ensuring that resulted distances are appropriate for ecological community datasets by down-weighting the influence of dominant taxa and excluding double absences as similarity (Legendre and Gallagher, 2001; Legendre and Legendre, 2012). While RDA remains a linear method, the transformation allows it to more effectively capture ecological relationships and makes it suited for a mix of taxon response shapes along environmental gradients. This approach avoids the limitations of a CCA, which assumes strictly unimodal taxon responses and disproportionately weights rare species due to its reliance on chi-squared distances, exaggerating their influence in the analysis (Legendre and Gallagher, 2001; Borcard et al., 2018). No transformation was applied for the indicator taxa analysis.

In a second step, we modeled the ecological niche of each chironomid taxon over the temperature gradient of our dataset to help in our interpretation of changes in downcore compositional data regarding summer temperature or other environmental influence potentially interfering with the reconstruction. We achieved this using logistic generalized additive models (GAMs) via the *gam()* function from the `MGCV` package (Wood, 2017), applied to occurrences data (binomial distribution). This approach avoids the dilution effect associated with relative abundance data, caused by variations of other taxa. For each taxon, summer temperature was used as the sole smoothing term in the model, or in a joint smooth with another environmental variable if the previous analyses indicated a secondary gradient influencing the taxon. Parameters were set on "REML" and a gamma (smoothness control) of two for every model.

Finally, we developed JJA temperature inference models on the newly modern dataset using two methods. The first one is the classical Weighted Averaging-Partial Least Squares (WAPLS; ter Braak and Juggins, 1993). The second one is an improved version of WAPLS proposed by Liu et al. (2020), hereafter *fxTWAPLS*, considering taxa tolerances and making a frequency correction for uneven sampling along the reconstructed variable gradient (Supplemental Fig. S4). The frequency correction consists of a weighting by the inverse frequency of the temperature value of the site during calculation of taxa scores (optima and tolerances) and for the regression of actual temperatures on the model components. Here, the frequencies were obtained by a binning of JJA temperature values in 1 °C increments (Supplemental Fig. S4), so that

each degree Celsius of the training-set gradient has the same weight in the inference model. In this method, the calculation of new temperature estimates includes a supplemental weighting of taxa abundances by the inverse square of taxa tolerances. Consequently, low-abundance stenothermic taxa will carry more weight than eurythermic taxa with high abundances in JJA temperature estimations from new assemblages. For more details about calculations used in *fxTWAPLS*, we refer to the original publication of this method. According to Liu et al. (2020), the *fxTWAPLS* should reduce the compression bias of WAPLS, allowing for more accurate inferences for climates outside the center of the gradient. We performed WAPLS using `RIOJA` package (Juggins, 2023) and *fxTWAPLS* with the second version of the function in `EXTWAPLS` package (Liu et al., 2020). We assessed performances of both inference models using 9999-Bootstrap cross-validation following the same procedure as in *crossval()* of `RIOJA` with the determination coefficient (R^2), the root mean square error of predictions (RMSEP) and the slope as assessing parameters. The slope represents the compression bias of the inference model with values nearest of 1 meaning almost no compression bias (Liu et al., 2020). The number of significant components was assessed by randomization (9999) t -tests (van der Voet, 1994).

We applied both inference models to the chironomid stratigraphy from Lake Igaliku, Lake Croche and Lake Mista. We calculated the sample specific errors (sse) using 9999 bootstraps for each reconstruction. For Lake Mista, we compared the new mean JJA air temperature reconstructions with the one based on mean August temperatures published by Feussom Tcheumeleu et al. (2023) using the 75-lake eastern Canadian transfer function (Bajolle et al., 2018; Larocque, 2008). We also looked at some reconstruction diagnostic elements of the Lake Mista record depending on the training-set used (the 182-lake set, or the 75-lake set), namely the relative part of fossil assemblages represented by taxa rare in the modern dataset ($N_2 < 5$), the analogue quality and the goodness-of-fit to temperature. We set quality threshold values as the 5th and 10th percentiles of squared-chord distances between all modern samples for the analogue quality and the 90th and 95th percentiles of squared residual lengths of modern samples for the goodness-of-fit. We set arbitrarily the threshold values as 10 and 20 % for the percent of rare taxa according to recommendations from (Brooks and Birks, 2001; Larocque-Tobler, 2010). We performed these diagnostics using *compare()*, *analogue_distances()* and *residLen()* functions from the package `ANALOGUE` (Simpson, 2007) and plotted with *autoplot()* from `GGPALAEO` (Telford, 2018). A R script for a shiny (Chang et al., 2024) app (Paleo-Recon Dashboard) allowing to reproduce cross-validation, reconstruction and diagnostics analyses is also available (see Data availability statement). We determined the zonation of the chironomid stratigraphic data of the Lake Mista by a CONISS clustering (Grimm, 1987) based on the Hellinger distance matrix of fossil samples with determination of the number of statistically significant zones by the broken stick model (Bennett, 1996). We applied smoothing cubic spline regression with default settings of *ss()* function from `NPREG` package (Helwig, 2024) on reconstructed temperature curves at the Lake Mista. Smoothing splines provide several advantages over fixed-span methods like LOESS, particularly for data with uneven temporal resolution. Unlike LOESS, which relies on an arbitrary fixed local span, smoothing splines adapt to the data structure by applying a penalty to excessive flexibility, resulting in a more balanced and data-driven fit (Simpson, 2018).

3. Results

3.1. Chironomid fauna distribution across latitudes and associated gradients

Aggregation of new data with existing data sets led to a new 182-lake training-set including 138 taxa, of which 100 occurred in at least two lakes with a maximal abundance reaching 2 % or more and were subsequently retained in the final training-set for data analyses. Overall, the modern distribution of the subfossil chironomid fauna in the dataset is

primarily related to the climatic gradient as indicated by the multivariate regression tree (MRT; Fig. 2), which has identified JJA temperatures of around 9 °C and 15 °C as main threshold values for lake assemblage partition. Lakes were classified in three main groups based on their chironomid assemblages that correspond to broad climatic zones, i.e. arctic, boreal, and temperate. The temperate lake group can also be further separated into “deep” (more than around 11 m) and “shallow” lakes (less than around 11 m) sub-groups.

A total of 49 taxa were identified as significant indicators of one or several groups of lakes from the MRT classification, resulting in the identification of 10 groups of indicator taxa (Table 2). Of these 49 taxa, 15 were associated to arctic environments (JJA <8.5 °C, e.g. *Heterotrissocladius*, *Micropsectra*, *Sergentia*, *Corynocera* ...), with 5 of them also indicator of boreal lakes (9 °C < JJA temp <15 °C), and 6 other taxa also associated to deep lakes in temperate conditions (JJA ≥ 15 °C and Depth ≥ 11 m); corresponding to the “Arctic”, “Arctic/Deep temperate”, “Arctic/Boreal”, and “Arctic/Boreal/Deep temperate” groups of indicator taxa. The warm side of the gradient holds 32 indicator taxa, belonging either to “Boreal/Temperate” or a strictly temperate group with 5 taxa showing also a preference for deep lakes and only *Zavreliella* favouring shallow lakes, the other warm indicators seem unaffected by the lake depth. This higher number of indicator taxa on the warm side of the training-set is consistent with the significant correlation between Hill’s N2 (effective diversity) and summer temperatures (Fig. 2; positive Pearson’s correlation with p-value <0.001 and adjusted R² = 0.32). Only *Constempellina/Thienemaniolla*, seemed strictly indicative of the intermediate temperature “Boreal” group while *Corynoneura* was classified as “undefined” because it does not exhibit any clear thermal preferences.

The RDA (Fig. 3) yields an adjusted R² of 19.2 % of the variance of the chironomid matrix explained by the environmental variables with all four canonical axes being significant (p-value <0.001) and

representing 16 % (RDA1), 3 % (RDA2), and 2 % (RDA3-4) of the variance, while the first residual axis (PC1) accounted for 8 % of the total variance. Therefore, RDA1 constitutes the most prominent variation axis within the structure of chironomid data. As this axis is primarily related to the temperature gradient with a secondary contribution of lake depth, it confirms the importance of these two variables in shaping assemblage composition as previously suggested by the MRT results. In addition, the first ordination plot (Fig. 3a) highlights the thermal preferences of some typical taxa associated with cold (on the left) and warm (on the right) conditions. All of them were also identified as significant indicators in the previous analysis.

Unlike the MRT, effects of conductivity and pH were noticeable on the third and fourth canonical axes of the RDA (both 1 % variance; Fig. 3b). However, only a few taxa seemed influenced by these two variables in the dataset. Variation partitioning (Fig. 4) further confirms the minor influences (less than 1 %) of conductivity and pH. Only summer temperature and to a lesser extent lake depth act as major environmental drivers of taxonomic composition of chironomid assemblages within our dataset.

3.2. Mean summer air temperature niche modelling

The results from logistic GAMs for the JJA air temperature niche of the 100 taxa are available in supplemental material appendix B and six illustrative examples are presented in Fig. 5. Taxa occurrence responses over the temperature gradient could be categorized into three main types: unimodal, monotonical and multimodal. Only few taxa exhibit a significant symmetric unimodal response curve to summer temperature, having almost no occurrences at both ends of the gradient. This is notably the case of *H. marcidus*-type, *Constempellina/Thienemaniolla* (Fig. 5), *Heterotanytarsus*, *Chaetocladius*, *C. oliveri*-type, *M. pallidula*-type,

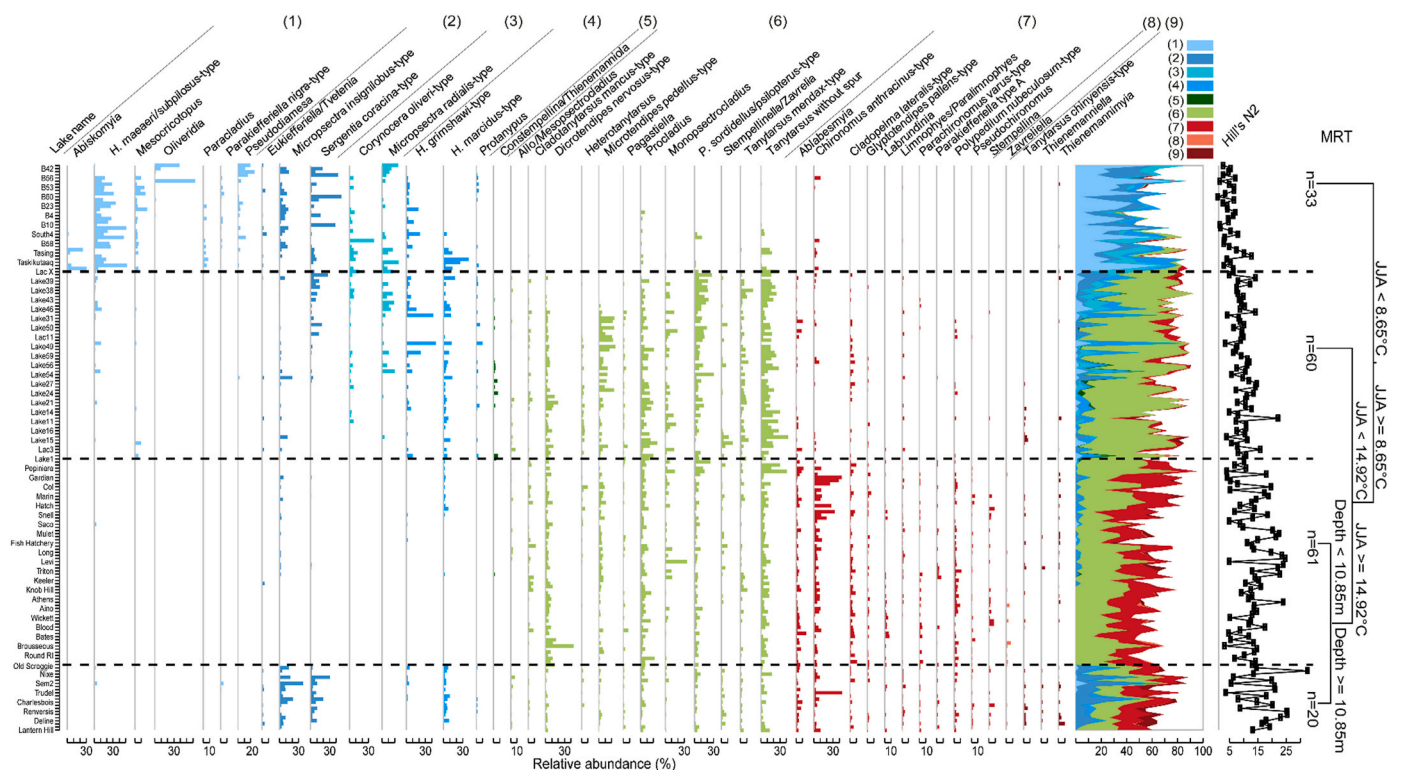


Fig. 2. Taxonomic composition of subfossil chironomid assemblages from surface sediment of the 182-lake training-set ordered according to a four groups MRT partition (CV error = 0.82 and SE = 0.02) and in increasing JJA temperatures from top to bottom within each zones; only taxa with a maximum of abundance of at least 5 % and identified as significant indicator taxa (p-value <0.05; see Table 2) of at least one group of the MRT clustering are shown; the colors correspond to the nine groups of indicator taxa identified by the *multipatt()* function (see Table 2), namely (1) Arctic, (2) Arctic/Deep, (3) Arctic/Boreal, (4) Arctic/Boreal/Deep, (5) Boreal, (6) Boreal/Temperate, (7) Temperate, (8) Temperate shallow, (9) Temperate deep. (For interpretation of the references to color in this figure legend, the reader is referred to the Web version of this article.)

Table 2

Significant indicator taxa (p.value < 0.05 after correction for multiple tests) on the four groups MRT partition of modern training-set's sites (IndVal values are indicated as square root). Crosses mean indicative value for the group of sites.

Taxa (morphotype)	JJA < 8.65 °C	JJA ≥ 8.65 °C JJA < 14.92 °C	JJA ≥ 14.92 °C; Depth < 10.85m	JJA ≥ 14.92 °C; Depth ≥ 10.85m	Indication	IndVal	p. value
<i>H. maeeri/subpilosus</i>	X	-	-	-	Arctic	0.91	0.01
<i>Mesocricotopus</i>	X	-	-	-	Arctic	0.83	0.01
<i>Pseudodiamesa</i>	X	-	-	-	Arctic	0.71	0.01
<i>Paracladius</i>	X	-	-	-	Arctic	0.64	0.01
<i>Parakiefferiella nigra</i>	X	-	-	-	Arctic	0.49	0.024
<i>Oliveridia</i>	X	-	-	-	Arctic	0.46	0.01
<i>Abiskomyia</i>	X	-	-	-	Arctic	0.39	0.048
<i>Micropsectra insignilobus</i>	X	-	-	X	Arctic/Deep temperate	0.81	0.01
<i>Sergentia coracina</i>	X	-	-	X	Arctic/Deep temperate	0.78	0.01
<i>Eukiefferiella/Tvetenia</i>	X	-	-	X	Arctic/Deep temperate	0.52	0.034
<i>Corynocera oliveri</i>	X	X	-	-	Arctic/Boreal	0.67	0.01
<i>Micropsectra radialis</i>	X	X	-	-	Arctic/Boreal	0.63	0.01
<i>Heterotrissocladius marcidus</i>	X	X	-	X	Arctic/Boreal/Deep temperate	0.73	0.01
<i>Heterotrissocladius grimshawi</i>	X	X	-	X	Arctic/Boreal/Deep temperate	0.73	0.014
<i>Protanypus</i>	X	X	-	X	Arctic/Boreal/Deep temperate	0.55	0.034
<i>Constempellina/Thienemanniola</i>	-	X	-	-	Boreal	0.59	0.01
<i>Procladius</i>	-	X	X	X	Boreal/Temperate	0.96	0.01
<i>Psectrocladius sordidellus-group</i>	-	X	X	X	Boreal/Temperate	0.94	0.01
<i>Tanytarsus</i> without spur	-	X	X	X	Boreal/Temperate	0.93	0.01
<i>Dicrotendipes nervosus</i>	-	X	X	X	Boreal/Temperate	0.91	0.01
<i>Microtendipes pedellus</i>	-	X	X	X	Boreal/Temperate	0.86	0.01
<i>Tanytarsus mendax</i>	-	X	X	X	Boreal/Temperate	0.8	0.01
<i>Monopsectrocladius</i>	-	X	X	X	Boreal/Temperate	0.73	0.01
<i>Stempellina/Zavrelia</i>	-	X	X	X	Boreal/Temperate	0.67	0.01
<i>Cladotanytarsus mancus</i>	-	X	X	X	Boreal/Temperate	0.63	0.014
<i>Pagastiella</i>	-	X	X	X	Boreal/Temperate	0.62	0.014
<i>All/Mesopsectrocladius</i>	-	X	X	X	Boreal/Temperate	0.6	0.034
<i>Heterotanytarsus</i>	-	X	X	X	Boreal/Temperate	0.58	0.038
<i>Ablabesmyia</i>	-	-	X	X	Temperate	0.86	0.01
<i>Chironomus anthracinus</i>	-	-	X	X	Temperate	0.86	0.01
<i>Polypedilum nubeculosum</i>	-	-	X	X	Temperate	0.84	0.01
<i>Cladopelma lateralis</i>	-	-	X	X	Temperate	0.79	0.01
<i>Labrundinia</i>	-	-	X	X	Temperate	0.74	0.01
<i>Limnophyes/Paralimnophyes</i>	-	-	X	X	Temperate	0.68	0.01
<i>Pseudochironomus</i>	-	-	X	X	Temperate	0.65	0.01
<i>Glyptotendipes pallens</i>	-	-	X	X	Temperate	0.63	0.01
<i>Parachironomus varus</i>	-	-	X	X	Temperate	0.61	0.01
<i>Tribelos</i>	-	-	X	X	Temperate	0.59	0.014
<i>Parakiefferiella-type A</i>	-	-	X	X	Temperate	0.56	0.014
<i>Lauterborniella</i>	-	-	X	X	Temperate	0.55	0.014
<i>Stempellina</i>	-	-	X	X	Temperate	0.53	0.014
<i>Paratendipes</i>	-	-	X	X	Temperate	0.51	0.024
<i>Synorthocladius</i>	-	-	-	X	Deep temperate	0.6	0.01
<i>Thienemannimyia</i>	-	-	-	X	Deep temperate	0.6	0.01
<i>Tanytarsus chinyensis</i>	-	-	-	X	Deep temperate	0.59	0.014
<i>Thienemanniella</i>	-	-	-	X	Deep temperate	0.56	0.01
<i>Phaenopsectra flavipes</i>	-	-	-	X	Deep temperate	0.43	0.018
<i>Zavreliella</i>	-	-	X	-	Shallow temperate	0.48	0.048
<i>Corynoneura</i>	X	-	X	X	Undefined	0.81	0.01

Paracladopelma, *T. chinyensis*-type and *T. lugens*-type, that tend to be more represented in the central part of the training-set. The other taxa had mainly an asymmetric distribution (unimodal or monotonical), either favoring the cold side or the warm side of the gradient. Asymmetric unimodal responses were characterized by decreasing occurrence probabilities at extreme values after passing an inflection point but without reaching null likelihood (Fig. 5; *Mesocricotopus* and *T. mendax*-type as examples), while monotonical responses reached a plateau of high occurrence probability over the end of the gradient (Fig. 5; *M. radialis*-type and *Labrundinia*). Not only the position of the inflection point (mode) or the plateau was different between taxa but also the slopes of the curves framing these points, leading to thermal niches characterized by their own temperature optimum and tolerance. A significant multimodal response was clearly found only for *Corynoneura*

(Fig. 5) and, to a lesser extent, for *M. insignilobus* (Supp. mat.).

For taxa influenced by lake depth or water chemistry (conductivity or pH), incorporating these variables in interaction with temperature yielded significant models. Response surfaces (Fig. 6 and supplemental materials) illustrate the preferences of taxa over gradients of the two variables. In most cases, the preferences for the two variables are superimposing themselves with a maximum of presence likelihood converging the optimum values for both variables.

S. coracina-type, *H. marcidus*-type, *M. insignilobus*-type and *C. anthracinus*-type have a true interaction between environmental variables because the pattern of temperature preferences is dependent on the value of the other variable. For instance, *S. coracina*-type displayed cold preferences in shallow lakes (<15m) but in deeper lakes (>15m) its occurrence remained at near-constant high probability on

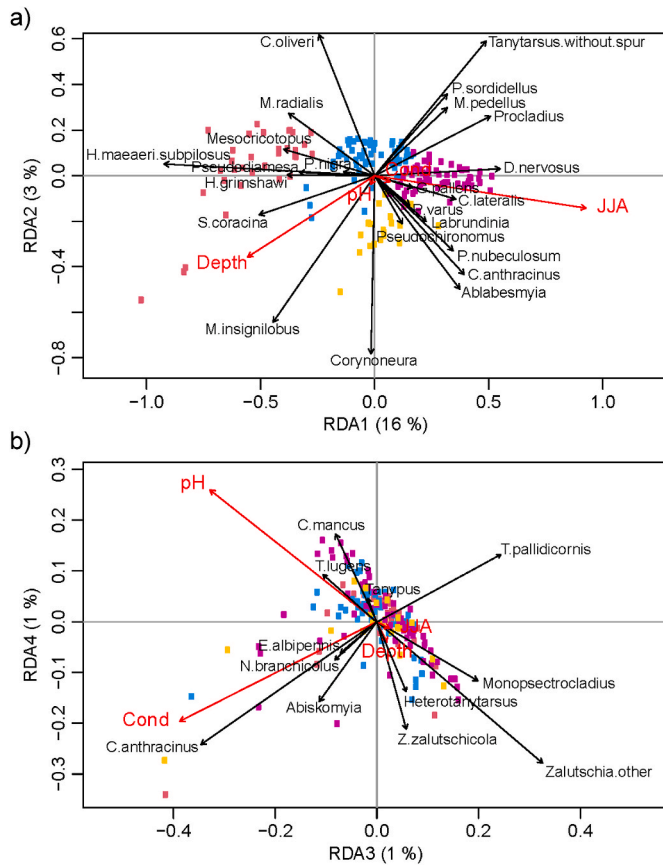


Fig. 3. RDA triplots of chironomid data constrained by environmental variables, namely mean June–July–August air temperature (JJA), conductivity (Cond), pH and lake depth (Depth); sites are colored according groups of the MRT partition (red squares JJA < 8.65 °C; blue squares JJA ≥ 8.65 °C and JJA < 14.92 °C; purple squares JJA ≥ 14.92 °C and Depth < 10.85m; yellow squares JJA ≥ 14.92 °C and Depth ≥ 10.85m). a) only taxa with a cumulated goodness-of-fit on RDA2 of at least 0.168 are shown; b) only taxa with a gain in cumulated goodness-of-fit from RDA2 to RDA4 of at least 0.0333 are displayed. These threshold values were set arbitrarily for displaying purpose of the main ecological relationships identified. (For interpretation of the references to color in this figure legend, the reader is referred to the Web version of this article.)

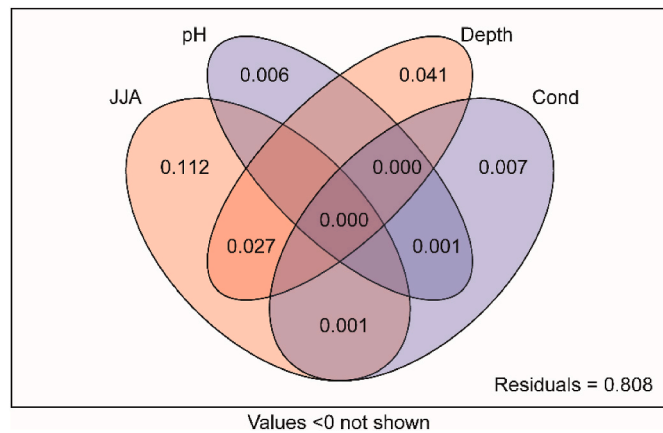


Fig. 4. Venn diagram of the chironomid assemblage’s data constrained by environmental variables; values are the relative part of variance represented by environmental variables.

the whole temperature gradient, thus extending the occupied temperature range. Therefore, the occurrence of *S. coracina*-type seemed air temperature related only in lakes less than 15 m deep. This is the same for *H. marcidus*-type (Fig. 6) and *M. insignilobus*-type (supplemental material) which are both able to occupy warmer lakes at higher lake depths. *C. anthracinus*-type also displays a similar phenomenon but with water conductivity, being positively responsive to temperature only at low levels of conductivity, otherwise the morphotype seems ubiquitous.

3.3. Cross-validation and independent assessment of inference models

Both inference models (WAPLS and fxTWAPLS) using two statistically significant components (p-value < 0.001) yield good performances in 9999-bootstrap cross-validation (Fig. 7 and Table 3). Yet, fxTWAPLS slightly outperforms WAPLS with a R² of 0.91 and a RMSEP (root mean square error of predictions) of 1.61 °C compared to 0.88 and 1.73 °C for classical WAPLS. Also, the slope of fxTWAPLS is closer to 1 (0.90), indicating a reduced compression bias compared to classical WAPLS which has a slope of 0.88. A closer look at the residuals (Fig. 7) shows a similar pattern for both models, with trends towards overestimation and underestimation at the cold end and the warm end of the gradient, respectively, but lower with fxTWAPLS. The improvement of temperature estimates with fxTWAPLS seems particularly true for cold inferences as the dispersal of residuals was considerably reduced compared to WAPLS for JJA temperatures less than 8 °C.

In a separate trial, we tested the removal of the 20 deep temperate lakes to reduce the influence of lake depth as a secondary gradient within the training-set. However, this did not improve the performance of either model. Consequently, we chose to retain all lakes in the transfer function dataset to better represent the ecological variability that may be encountered in potential study sites.

Stratigraphic diagrams of the chironomid records from Lake Igaliku and Lake Croche are presented in supplemental materials (Supplemental Figs. S5 and S6). In both lakes, a substantial portion of the downcore subfossil assemblages consisted of key indicator taxa listed in Table 2. This resulted in cumulative plots of indicator groups (Fig. 8) that closely align with their climatic positions within the full spectrum of the calibration dataset (Fig. 2). For the Lake Igaliku, this means assemblages composed of few taxa dominated by “Arctic”-linked categories (*Microprospectra* and *Heterotrissocladius*) with a non-negligible part of “Boreal/Temperate” (*Dicrotendipes* and *Psectrocladius*), typical of assemblages at the transition between the “Arctic” and “Boreal” zones on Fig. 2 which correspond to the actual temperatures of this site (JJA from 8 °C to 10 °C). For the Lake Croche, the taxon-rich downcore assemblages dominated by indicator taxa belonging to the “Boreal/Temperate” and “Temperate” groups along with a lesser contribution of taxa associated to the “Temperate deep” group are characteristic of deep temperate lakes matching both mean JJA air temperatures (around 17 °C) and maximal depth (11.4m) of the site. The sample scores on the first axis of principal component analyses (PCA) of subfossil chironomid matrices were significantly correlated with JJA temperatures only for Lake Igaliku (p-value < 0.01, adjusted R² = 0.52), whereas no significant correlation was found for Lake Croche (p-value = 0.8).

Overall, applying our inference models on recent stratigraphy yields temperature reconstructions close to instrumental records (Fig. 9). For Lake Igaliku both WAPLS and fxTWAPLS provide inferences significantly correlated to meteorological values (Table 3) but inferences from WAPLS are affected by a systematic overestimation of 1–2 °C while fxTWAPLS-based inferences were closer to the actual temperatures resulting in a lower RMSEP (0.93 °C) for this method, in addition of having a better R² (0.63). For Lake Croche, there is no significant correlation between meteorological and chironomid-inferred temperatures regardless of the inference methods, however almost all instrumental values are within the model error on each inference, resulting in low RMSEP for both models (0.76 °C and 0.64 °C respectively for WAPLS and fxTWAPLS).

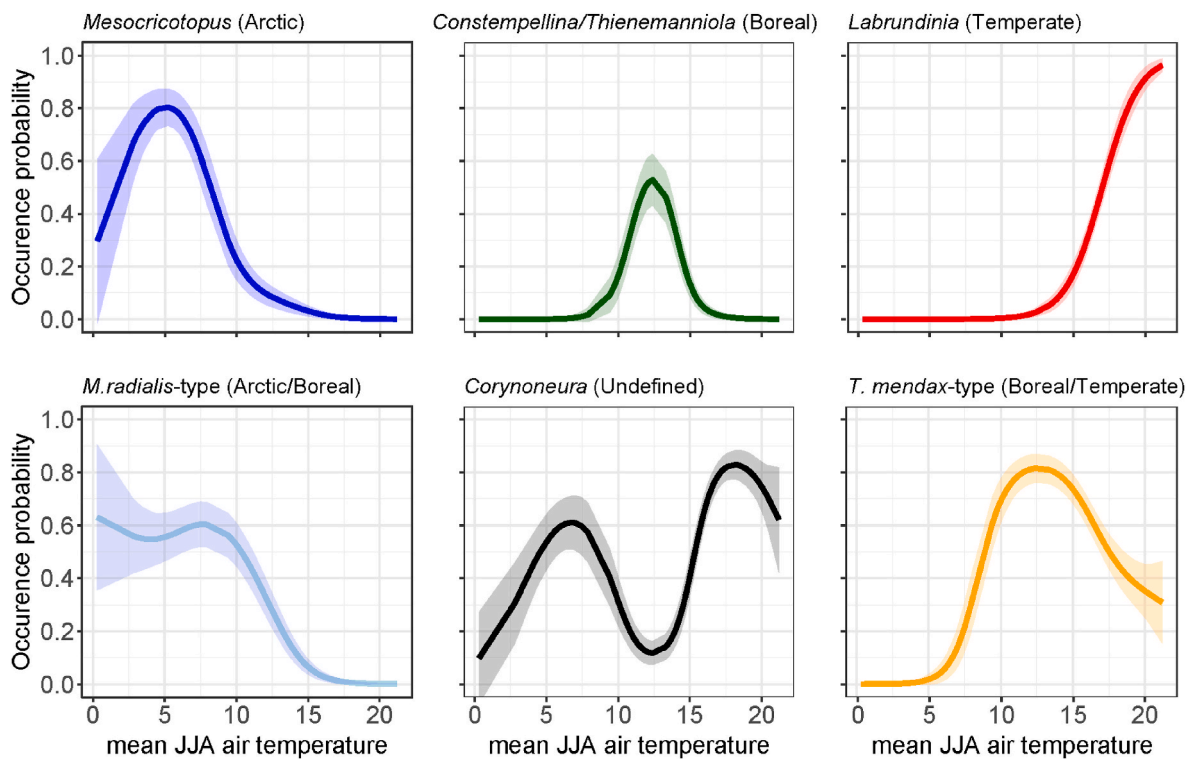


Fig. 5. Realized summer air temperature niche of some indicator taxa (Table 2) generated by logistic GAMs; JJA was significant (p -value < 0.05) as smoothing term in all of these models; the taxa chosen here are examples of cold asymmetric unimodal (dark blue), cold asymmetric monotonical (light blue), symmetric unimodal (green), multimodal (black), warm asymmetric monotonical (red) and warm asymmetric unimodal (yellow) response curve shape over the temperature gradient. (For interpretation of the references to color in this figure legend, the reader is referred to the Web version of this article.)

3.4. Postglacial trends of summer air temperatures inferred at Lake Mista

Stratigraphy of subfossil chironomid assemblages from Lake Mista core are presented in Feussom-Tcheumeleu et al. (2023) and in supplemental material (Fig. S7). The cumulative spectrum of indicator taxa identified in Table 2, effective diversity (Hill's N2) and fossil scores on PCA first axis (24.9 % of the total variance; Hellinger distance based) are presented in Fig. 10. According with the broken stick model, four statistically significant biozones can be derived from the coniss clustering of fossil assemblages. Briefly, chironomid assemblages after the glacier retreat from 8500 BP to 8000 BP were dominated by cold-indicator taxa associated to the arctic and the boreal zones, or with a high lake depth (*Sergentia*, *Micropsectra*, *Heterotrissocladius marcidus*-type and *C. oliveri*-type). However, only a very negligible proportion of the taxa inhabiting the lake were strictly indicator of arctic conditions. Nowadays, similar assemblages are found near the cold end of the boreal zone in lakes with sufficient depth (Fig. 2). Shortly after 8000 BP the abundance of those cold-indicator taxa declined, remaining the only taxa able to substitute cold climate by lake depth (i.e. Arctic/Deep temperate and Arctic/Boreal/Deep temperate indicators). "Boreal/Temperate" indicator taxa closely followed by "Temperate" indicator taxa both reached their maximum abundances during the mid-Holocene between 7000 BP and 4200 BP, coinciding with the highest Hill's N2 values recorded. This pattern aligns with the warmer summers characteristic of the Holocene Thermal Maximum (HTM). At the beginning of the Late-Holocene (around 4200 BP), warm-associated taxa started to slightly decrease while some cold-associated taxa slowly recovered, including *C. oliveri*-type and *T. lugens*-type, both of which had almost disappeared from the lake during the mid-Holocene. This taxa turnover indicates the onset of the cooling trend of the Neoglacial period for the last 4000 years BP, although it was interrupted by an increase in the relative abundance of the temperate indicator *Ablabesmyia* (Table 2) between 2500 and 2000 BP. The last 1500 years are characterized by the occurrence of

C. oliveri-type and the substantial increase of *M. insignilobus*-type percentages reaching 30 %, while "temperate" taxa almost disappeared and relative abundance of "boreal/temperate" taxa is strongly reduced. This coincides with the lowest Hill's N2 values of the whole record. It is noteworthy that fossil PC1 scores had similar variations with changes of relative abundances of indicator taxa groups as well as the Hill's N2 (Fig. 10).

Diagnostic elements indicate that fossil chironomid data from Lake Mista has a good potential to produce a high-quality JJA temperature reconstruction when applied with the new 182-lake training-set (Fig. 11, right panels). Indeed, the quality of the record is good or fair for most samples according to the three diagnostics altogether. For comparison, 5–30 % of fossil assemblages are taxa with less than five effective occurrences in the surface dataset of the Eastern Canadian transfer function used in Feussom-Tcheumeleu et al. (2023) (Fig. 11, left panels). This lack of common abundant taxa between fossil data and this previous training-set version resulted in poor analogue quality for almost all samples. Nevertheless, around two thirds of fossil assemblages had a good fit to temperature.

The new 182-lake training-set and its two associated inference models (WAPLS and fXTWAPLS) applied to the Lake Mista record produce quantitative mean JJA air temperature reconstructions with a general pattern like the mean August reconstruction of Feussom Tcheumeleu et al. (2023) (Fig. 12). The initial warming after the glacier retreat was followed by a warm mid-Holocene and a cooling trend over the late-Holocene. This last cool period was interrupted by a warming episode between 2500 and 2000 BP. However, inferred temperature values and magnitudes of changes are quite different between the three reconstructions. Specifically, using the 182-lake training-set produce warmer temperature reconstruction during the mid-Holocene with JJA anomalies of +3 to +4 °C, while the mean August reconstruction indicated +2 °C. As a result, the cooling trend at the start of the late-Holocene is steeper with the new training-set and the warming

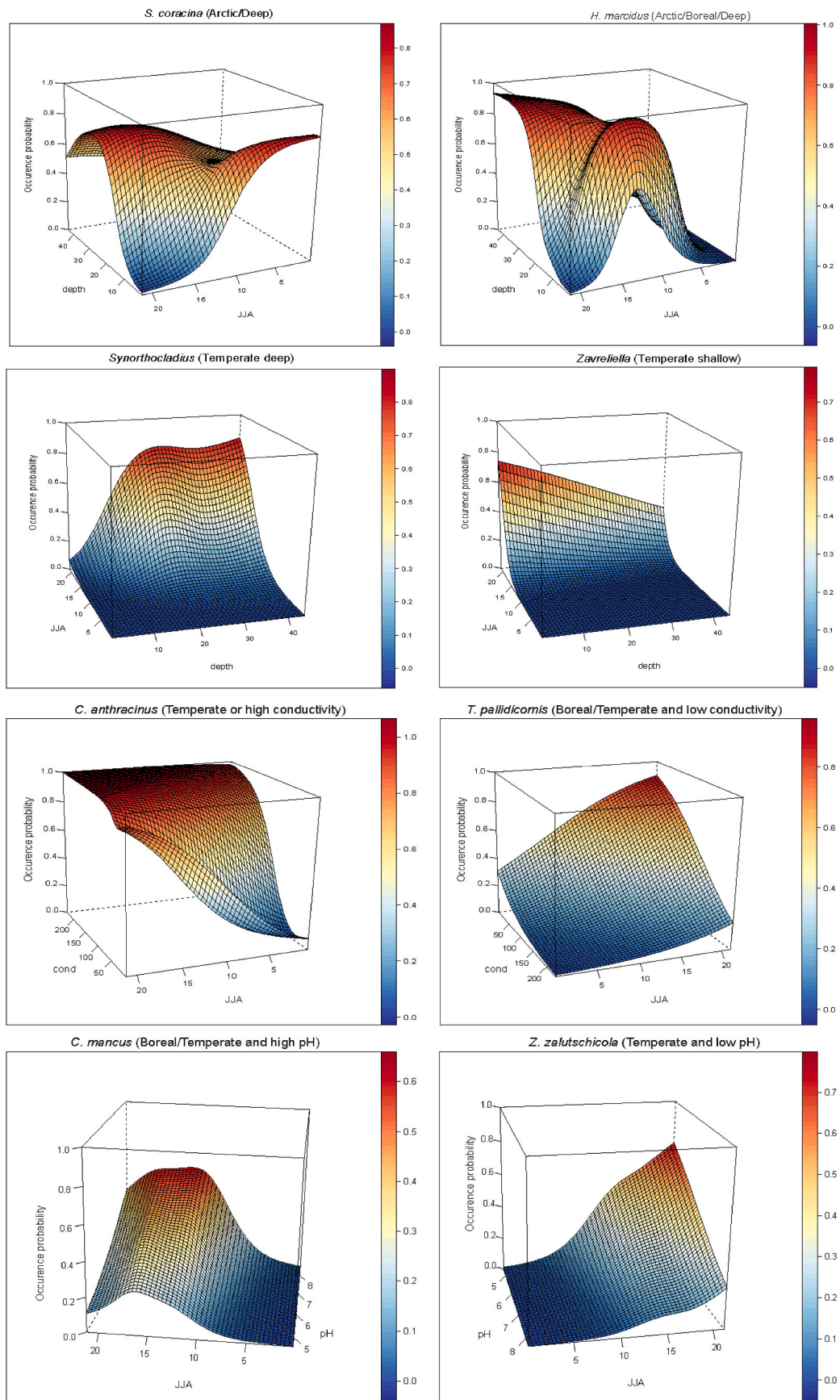


Fig. 6. Response surface to summer temperature gradient with another environmental variable of some taxa showing an influence of lake depth, conductivity or pH generated by logistic GAMs; all models presented here are significant (p -value < 0.05) with the interaction of the two variables as a smoothing term.

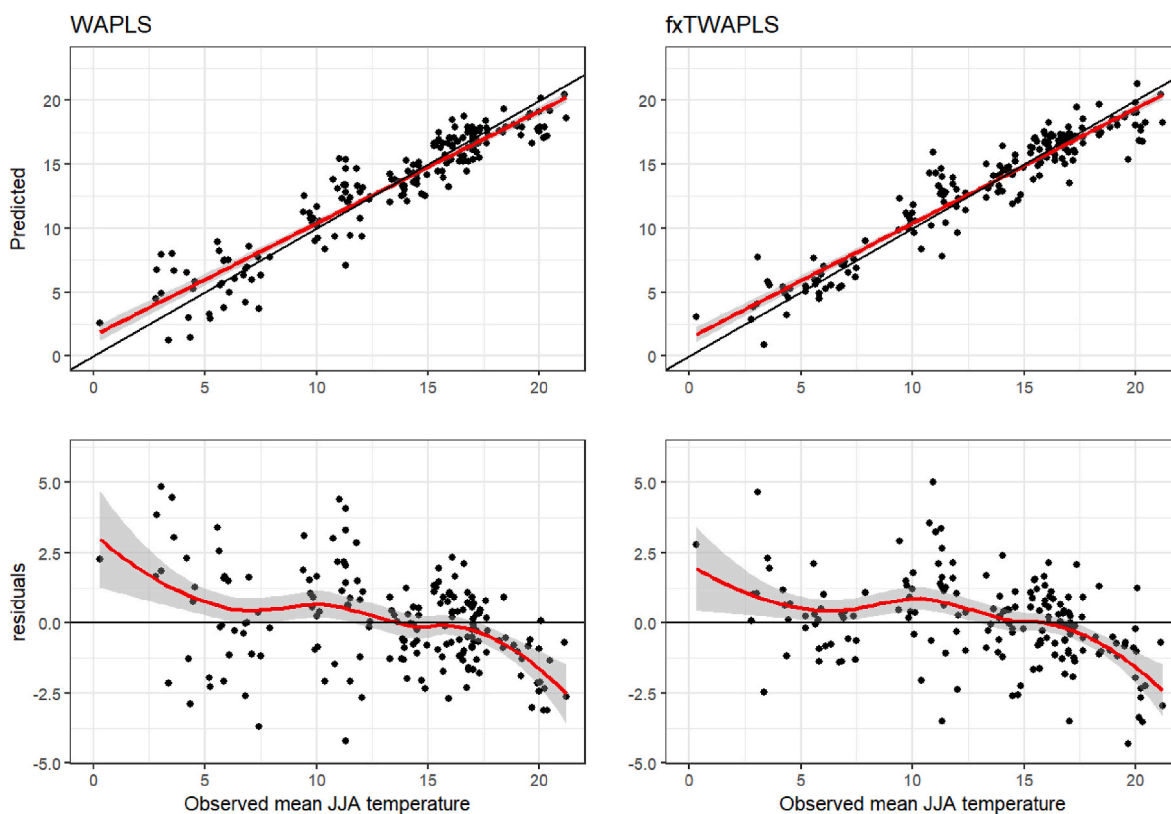


Fig. 7. 9999-Bootstrap cross-validation results for WAPLS (left) and for fxTWAPLS (right); red lines are linear regression (top) and loess smoothing curves (bottom); residuals are calculated as chironomid-inferred temperature less actual mean JJA air temperature. (For interpretation of the references to color in this figure legend, the reader is referred to the Web version of this article.)

Table 3

Performances of the inference models according to 9999-Bootstrap cross-validation (see Fig. 7) and comparison to meteorological records on the cores from Lake Igaliku and Lake Croche (see Fig. 9). NA means non applicable because of non-significance of linear models.

		WAPLS (2 components)	fxTWAPLS (2 components)
Cross-validation	R ²	0.88	0.91
	Slope	0.88	0.90
	RMSEP (°C)	1.73	1.61
	% gradient	8.28	7.70
Lake Igaliku	r (pearson)	0.74	0.81
	p-value	0.002	<0.001
	R ²	0.51	0.63
	RMSEP (°C)	2.08	0.94
Lake Croche	r (pearson)	0.17	0.27
	p-value	0.55	0.34
	R ²	NA	NA
	RMSEP (°C)	0.76	0.64

period of 2500-2000 BP more clearly defined. There are also some differences between the new training-set WAPLS-based reconstruction and the fxTWAPLS-based one. Mainly, fxTWAPLS extends the reconstructed temperature range with both warmer and colder inferences than the WAPLS-based ones. The fxTWAPLS-based reconstruction is the only one to show distinct colder-than-today periods following the retreat of the Laurentian ice sheet and toward the end of postglacial history, aligning with the so-called Little Ice Age (LIA).

4. Discussion

4.1. Summer temperatures drive chironomid assemblage composition

Our results show a strong empirical link between summer temperature and chironomid assemblage composition. Canonical analyses confirmed that mean summer air temperature and secondarily lake depth, act as major drivers of the distribution of chironomid taxa in the surface sediment of the 182 lakes. Nearly half of the chironomid taxa had a significant indicative value for one or two zones of the JJA temperature gradient partitioned by MRT (Table 2; arctic, boreal, and temperate). Niche modelling (Fig. 7 and supp. mat. app. B) produced numerous significant responses of taxa occurrence to JJA temperatures with shapes that are expected for an ecologically important gradient according to niche theory (Hutchinson, 1957; Whittaker et al., 1973), namely a near-gaussian unimodal response that appears as monotonical for taxa with optima outside the sampled temperature range. These results show the strong link between chironomid assemblages and summer temperatures at a broad geographical scale and support the relevance of subfossil chironomids as proxies for the quantitative reconstruction of past summer temperatures. This finding is in close agreement with previous studies of large scale chironomid distribution in lake sediment from various areas around the world that showed a strong relationship between temperature and taxonomic composition of subfossil assemblages (Nearctic: Fortin et al., 2015; Griffiths et al., 2024; Porinchi et al., 2007; Palearctic: Bakumenko et al., 2024; Engels et al., 2020; Heiri et al., 2011; Nazarova et al., 2015; Afrotropical: Eggermont et al., 2010; Neotropical: Matthews-Bird et al., 2016; Motta and Massafiero, 2019; Wu et al., 2015; Australasia: Rees et al., 2008; Woodward and Shulmeister, 2006).

We detect only minor effects of water chemistry variables on chironomid assemblage variability, and they tend to be restricted to a

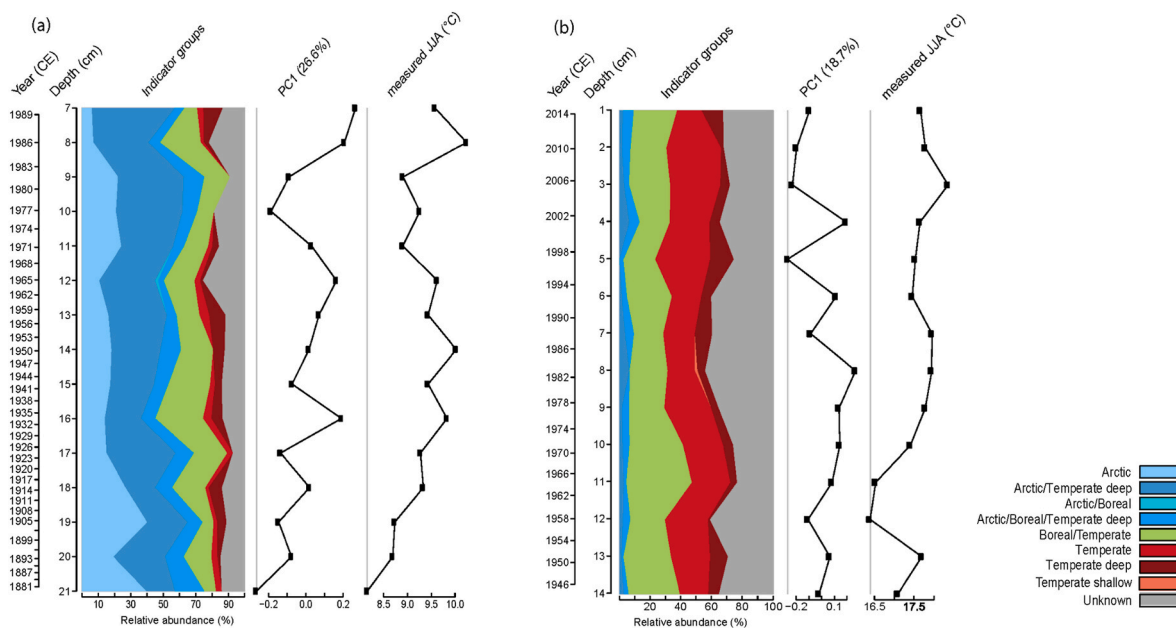


Fig. 8. Indicators spectra of subfossil records from Lake Igaliku (a) and Lake Croche (b) along scores on the first components of principal component analyses (PC1) applied on each chironomid matrix and measured JJA temperature from weather stations. PC1 is significantly correlated with measured JJA temperatures for the record of Lake Igaliku (p -value<0.01; adjusted $R^2 = 0.52$) and the same relationship is statistically non-significant in record of Lake Croche (p -value = 0.8).

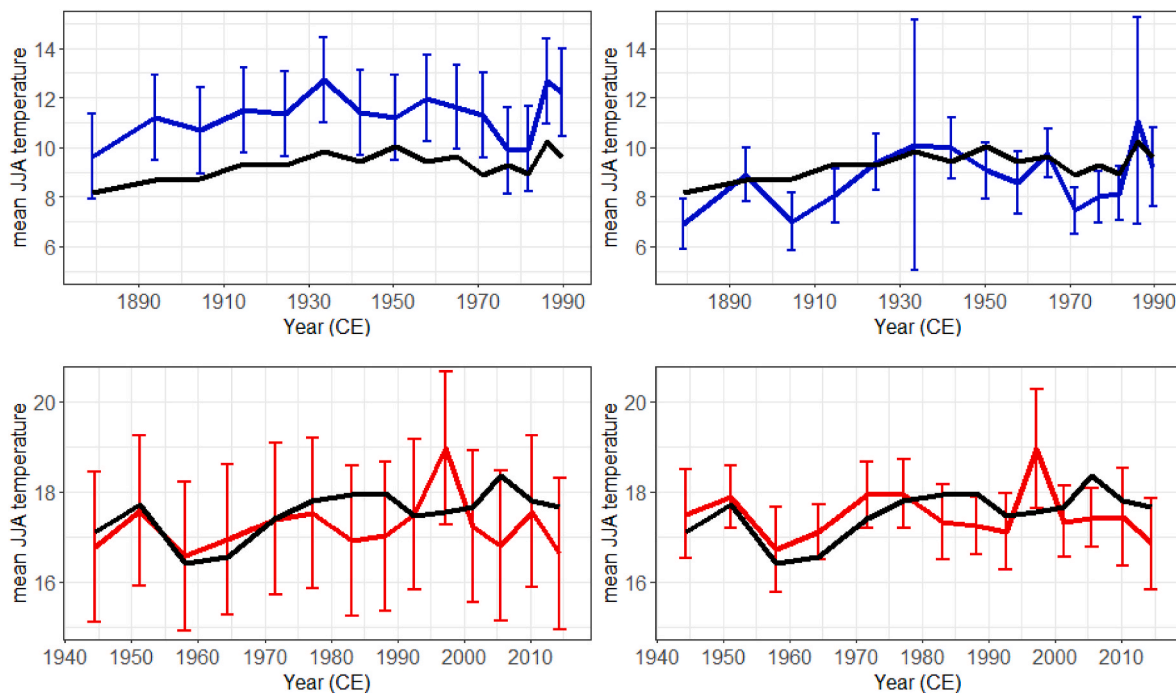


Fig. 9. Comparison between meteorological records (black lines) and chironomid-inferred temperatures on the cores from Lake Igaliku (blue lines) and Lake Croche (red lines); left panels are results with WAPLS and right panels with fXTWAPLS. (For interpretation of the references to color in this figure legend, the reader is referred to the Web version of this article.)

limited number of taxa such as *Tanytarus pallidicornis*-type associated with low conductivity (Cao et al., 2019) or typical taxa of dystrophic conditions like *Zalutschia*, *Heterotanytarsus* and *Monopsectrocladius* for low pH values (Walker et al., 1985; Walker and Paterson, 1983). *Cladotanytarus mancus*-type could have a possible sensitivity to acidification, as previously indicated by Bilyj and Davies (1989) for some species of the same genus.

Typical genera and morphotypes of warm and cold conditions found

in our training-set have analogue thermal preferences compared to other training-sets from the Nearctic (Barley et al., 2006; Medeiros et al., 2022; Porinchi et al., 2007) and the Palearctic (Hamerlík et al., 2017; Heiri et al., 2011; Kotrys et al., 2020; Larocque et al., 2001; Nazarova et al., 2015). The overall succession order along the latitudinal gradient of our study is also echoed in Chironomidae distribution along the river continuum (Rossaro, 1991; Rossaro et al., 2022). Although the absolute values of the thermal optima of the different taxa may vary from one

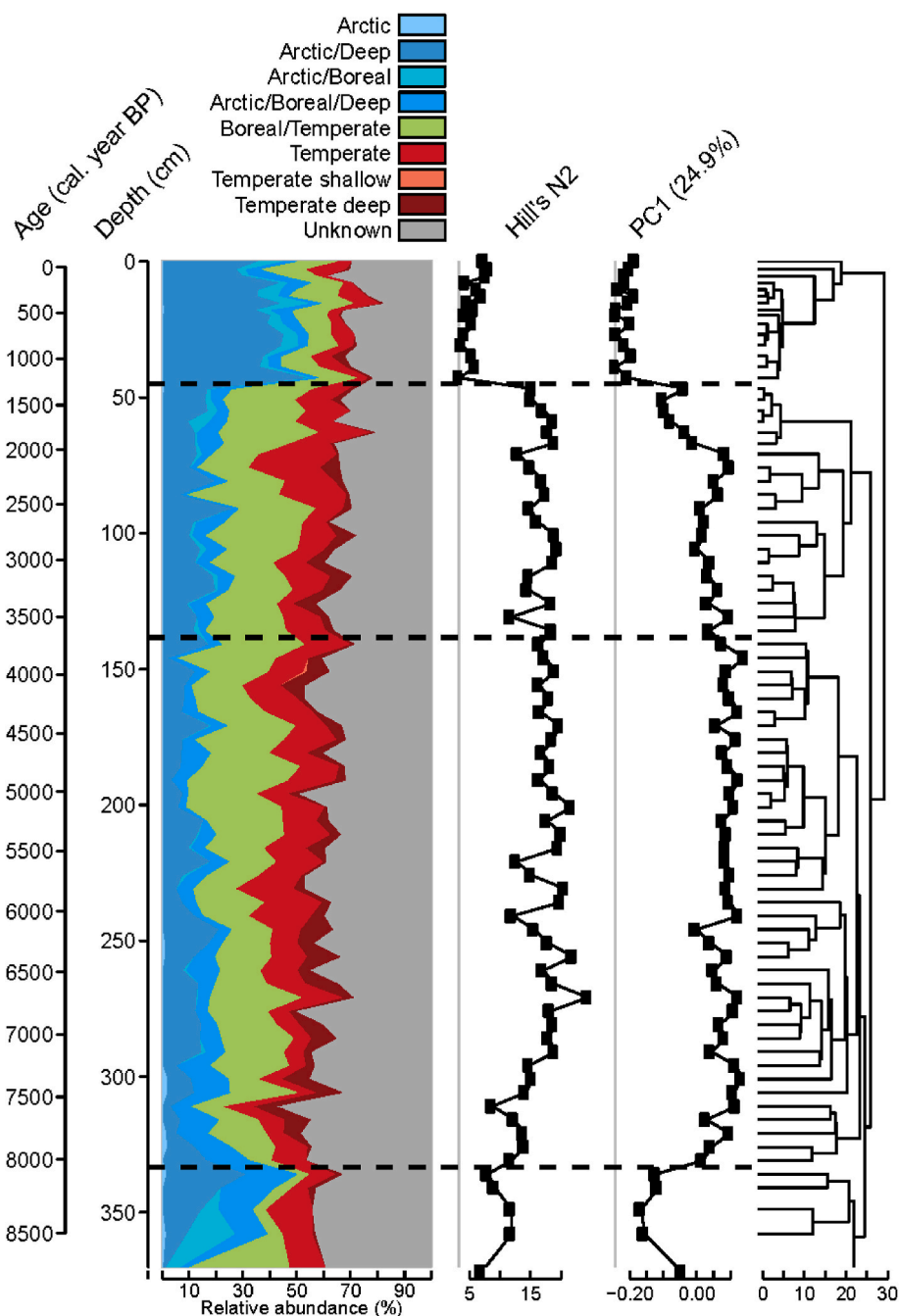


Fig. 10. Spectrum of cumulative percentages of indicator taxa from the record of Lake Mista with the Hill's N2 ("effective diversity") of assemblages and scores of samples on first component of PCA along core depth and samples estimated ages with sequential CONISS clustering.

study to another (depending on the geographical area and calculation method), the succession of taxa along the thermal gradient are remarkably similar and concordant.

This overall consistency does not mask certain differences in the thermal preferences of some taxa between our dataset and previous studies. For instance, *Parakiefferiella* type A was quite recurrent in surficial sediments of temperate lakes in our dataset, being even a significant indicator of the group, while it was found in Younger Dryas sediments (glacial-like conditions) in Switzerland (Brooks, 2000; Heiri, 2001). Another example is the predominantly Neotropical genus *Labrundinia* (Da Silva et al., 2014), which is represented in Europe by only one species most abundantly found in bogs (Brooks et al., 2007), while from our dataset the genus appears to be a common indicator of the warmest part of the gradient (Table 2; Fig. 7).

The apparent uniformity of the empirical chironomid-air temperature relationships across lakes and other temperature-related aquatic gradients (rivers) in the Holarctic region indicates the ecological significance of the underlying temperature-associated mechanisms for the chironomid fauna (cf. Juggins, 2013). Moreover, these relationships are apparent at the genus level meaning that thermal preferences are probably ancient and quite resistant to small evolutionary changes, explaining the overall transcontinental ecological equivalence of chironomid taxa that are phylogenetically close regarding temperature preferences (Larocque-Tobler, 2010; Lotter et al., 1999). This feature allows the use of "space-for-time calibration" on hundreds of thousands of years with no major deterioration in reconstruction performance (Axford et al., 2011; Bolland et al., 2022; Francis et al., 2006; Pliikk et al., 2019; Rigterink et al., 2024) that would have come from evolutionary

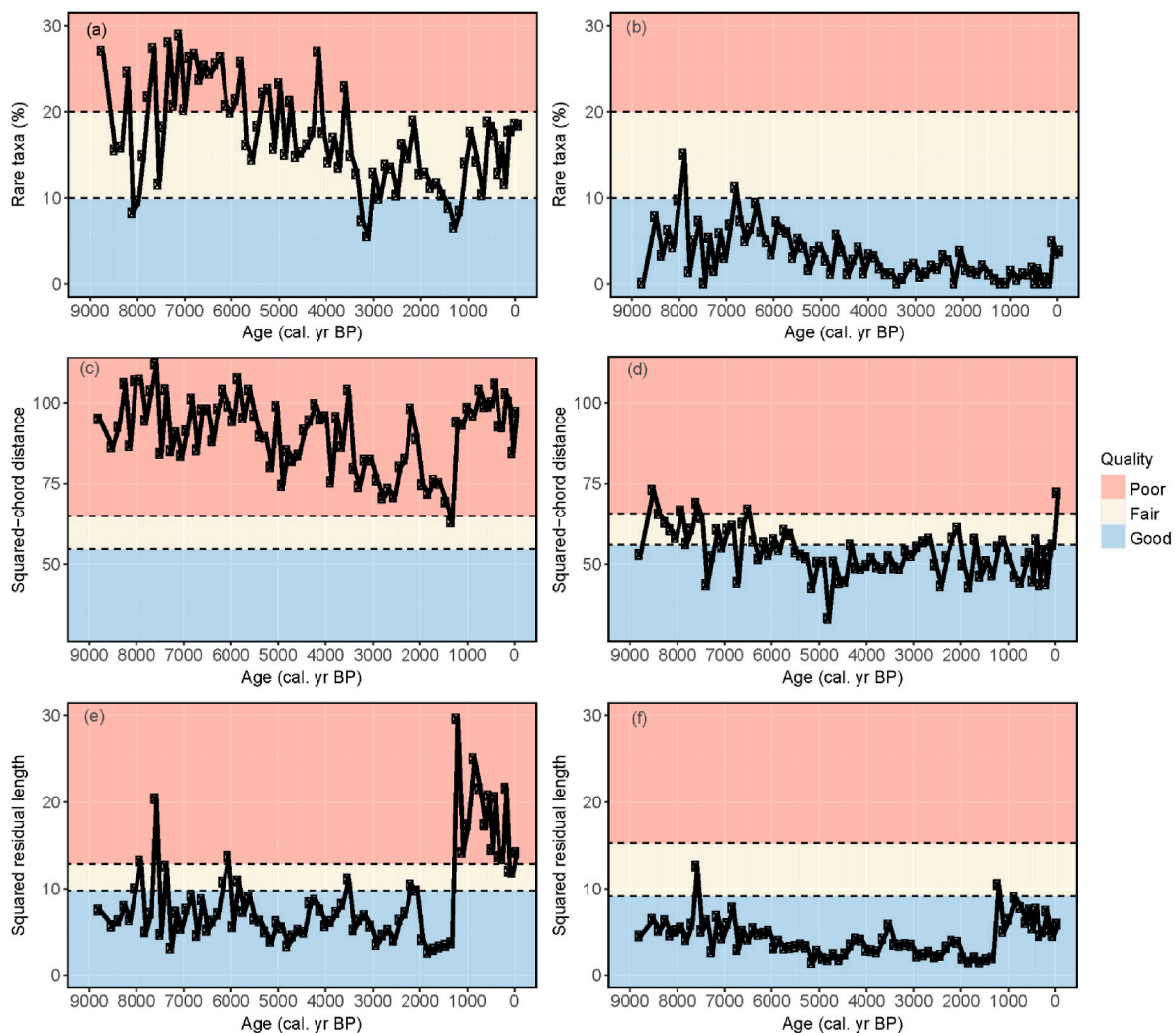


Fig. 11. Reconstruction diagnostic elements applied on the chironomid record from Lake Mista; Left panels are results with the northwestern Quebec training-set used in Feussom Tcheumeleu et al. (2023) and right panels with the 182-lake training-set of this paper; (a–b) Cumulated relative abundance of rare taxa in the modern dataset ($N_2 < 5$) within fossil samples; (c–d) Analogue quality represented by the squared-chord distance between fossil assemblages and their closest modern assemblage, threshold values are set as the 5th and the 10th percentiles of squared-chord distances between all modern assemblages; (e–f) Goodness-of-fit to summer temperature of fossil samples, represented by the squared residual length of fossil samples passively added to a CCA ordination of modern samples constrained by summer temperatures, threshold values are set as the 90th and the 95th percentiles of squared residual lengths of modern samples.

changes of thermal preferences.

4.2. Direct physiological constraints of water temperature

Though empirically strong, the underlying mechanisms of the chironomid-temperature relationship are not fully understood, mainly because of their complex nature. Chironomid larvae integrate in-lake conditions, with air temperatures—strongly influencing surface water temperatures (Livingstone and Lotter, 1998)—affecting chironomids through a complex interplay of direct physiological impacts and indirect ecosystem effects (Eggermont and Heiri, 2012).

It is difficult to decipher with only observational distribution data if a taxon response to a summer air temperature gradient is more constrained by its physiological requirements for water temperature or by indirect influences. Nonetheless, experimental studies have demonstrated the importance of water temperature for the physiology of chironomid immature stages. For instance, exposure of cold-stenotherms to warm temperatures results in mortality, while eurythermic taxa require a minimum level of warmth to complete their life cycle, even if larvae can survive cold temperatures during overwintering (Balci and Kennedy, 2002; Brodersen et al., 2008; Dickson and Walker,

2015; Lencioni et al., 2008). In this sense, cold indicators are more physiologically constrained in their distribution by water temperature and can be considered true stenotherms, while indicator taxa of warm conditions in mid-latitude still must survive to cold temperatures during larvae overwintering and therefore have a broader physiological tolerance regarding water temperature.

In our dataset, cold-stenothermic taxa such as *Sergentia coracina*-type, *Micropsectra insignilobus*-type, *Heterotrissocladius marcidus*-type and *grimshawi*-type and *Protanypus*, can thrive either in arctic climate, or in warmer climates if lake depth is sufficiently important (Table 2; Fig. 8 and supp. mat.). Due to thermal stratification, cold hypolimnetic waters of lakes with sufficient depth can function as a thermal refugium for cold-water taxa able to develop in sublittoral and profundal lake conditions. These taxa can be referred as “eurybathic psychrostenothermic” (Hofmann, 1971, 1988). Indeed, those taxa can inhabit shallow depths in the arctic (Aagaard, 1986; Brundin, 1949) and also constitute the “*Tanytarsus lugens* community” (Brinkhurst, 1974; Brundin, 1956; Saether, 1975, 1979; Thienemann, 1920) in the profundal zones of stratified oligo to mesotrophic lakes under temperate climate conditions, more specifically the *Micropsectra*-association in oligotrophic lakes (Frossard et al., 2013; Gerstmeier, 1989; Lods-Crozet and

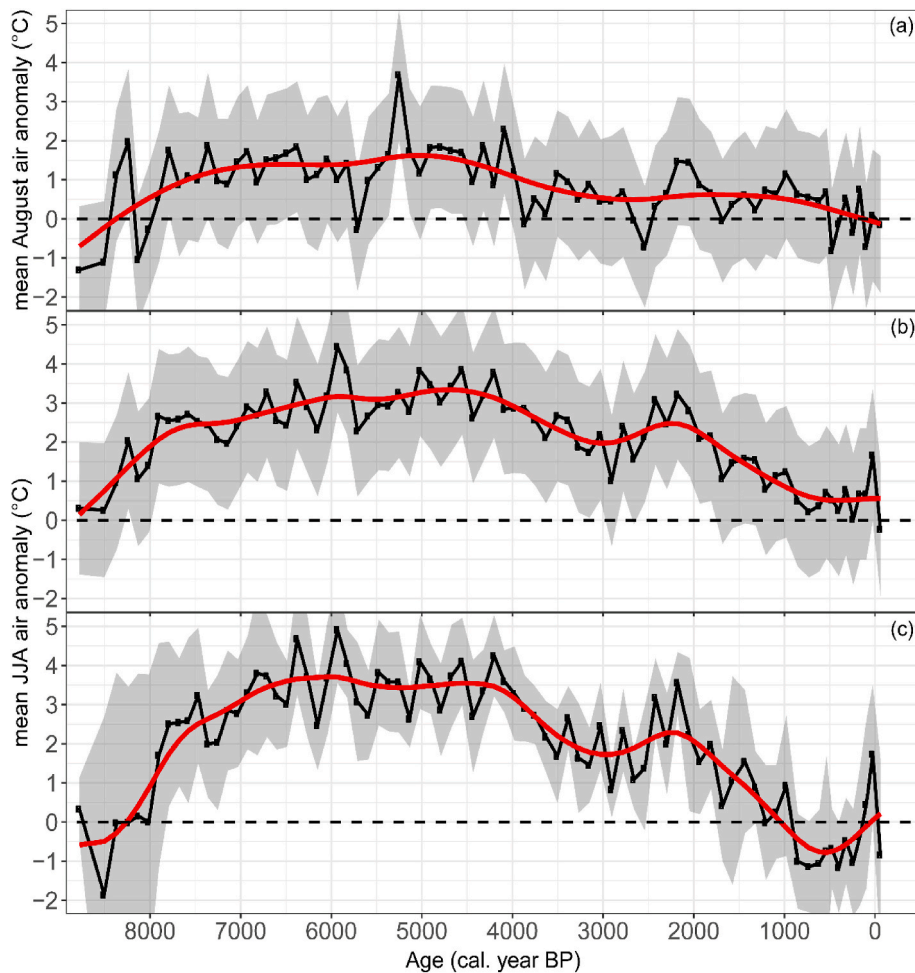


Fig. 12. Chironomid-inferred temperature reconstructions plotted on mean ages of the postglacial core from Lake Mista; a) original WAPLS-based mean August air temperature data from Feussom Tcheumeleu et al. (2023), ages were updated with the new Bayesian age-depth model; b-c) mean JJA air temperature reconstruction by WAPLS (b) and fXTWAPLS (c) with the new 182-lake modern calibration dataset of this paper; a-b-c) red lines are smoothing cubic spline of temperature inferences and grey areas represent the bootstrap sample specific error. (For interpretation of the references to color in this figure legend, the reader is referred to the Web version of this article.)

Lachavanne, 1994; Millet et al., 2010), *Sergentia*-association in mesotrophic lakes (Belle et al., 2016, 2017; Brundin, 1958; Stahl, 1966) or even *Heterotrissocladius* dominance in the Great Lakes (Winnell and White, 1986). Consequently, the statistical power of lake depth in canonical analyses, which is primarily the differentiation between deep temperate lakes that host eurybathic psychrostenothermic taxa and unstratified shallow lakes (only warm-adapted taxa), is functionally a response of the chironomid fauna to a local temperature gradient governed by the lake thermal regime (Quinlan et al., 2012).

The influence of hypolimnetic cold water could also be beneficial for taxa such as *Eukiefferiella*/*Tvetenia*, *H. marcidus*-type, *Synorthocladius*, *Phaenopsectra flavipes*-type, *Thienemannimyia* and *Thienemaniella* which are more commonly considered as typical for spring-fed and headwater conditions in rivers (Brooks et al., 2007; Loskutova et al., 2023; Rossaro et al., 2022). Indeed, preferences for colder and more oxygenated water would explain why they are indicators of deep temperate lakes in our dataset. In brief, it would be more appropriate to consider “profundal” and “lotic” taxa as true indicators of water temperature and oxygenation, rather than being dependent on a specific aquatic habitat (lentic vs. lotic, or littoral vs. deep). Therefore, in summer air temperature reconstructions, taxa with physiological limitations for cold water temperatures should be interpreted based on the origins of these water conditions in the lake. These conditions may result from various combinations of climate and lake thermal regimes, as well as specific

hydrological features such as groundwater and meltwater inputs (Brooks and Birks, 2001; Jennings, 2021; Lindegaard, 1995) or even topographical shading (Hamerlík et al., 2017; Novikmec et al., 2013). In deep stratified lakes, a cold hypolimnion ensures physiological requirements for water temperature of cold-stenothermic taxa and their distribution becomes constrained by hypolimnetic oxygenation (Quinlan and Smol, 2001), which can in turn be influenced by effects of summer air temperatures on lake productivity and thermal regime, making abundances of those taxa still responsive to air temperatures through indirect influences.

4.3. Indirect ecosystem effects of mean summer air temperature

Eggermont and Heiri (2012) outlined the importance of indirect effects of air temperatures on chironomids through their effects on lake functioning. This kind of influential pathway is illustrated in our data by the conductivity-dependent thermal niche of *Chironomus anthracinus*-type (Fig. 6). This genus characterizes profundal communities of oxygen-depleted eutrophic lakes (“*Chironomus* lake”; Brundin, 1956, 1949; Hofmann, 1988; Saether, 1979, 1975; Thienemann, 1954, 1920), therefore it can thrive within the cold hypolimnetic waters (4–6 °C) and its few occurrences in some Arctic lakes suggest that cold water temperature is not a limiting factor of its distribution. Despite this physiological tolerance for cold temperatures, *C. anthracinus*-type exhibits a

thermophilic value in our training-set being indicator of temperate lakes where it can be quite abundant, representing up to 30 % of surface assemblages.

Distribution of *C. anthracinus*-type seems to be unrelated to water temperature and its distribution preference for lakes with warm JJA air temperature would be the result of its high saprobic value since there are overall correlations between air temperature, nutrient availability, conductivity, and organic matter in the sediment (Brodersen and Anderson, 2002; Medeiros and Quinlan, 2011; Velle et al., 2010). Dranga et al. (2018) show that conductivity is mainly defined by bedrock and physiographic settings and higher conductivity is often accompanied by more nutrients, leading to higher trophic status and then more organic matter into sediments. However, lake productivity is also driven positively by summer temperature and tree cover, which would compensate for low nutrient input from watershed of low conductivity. This could explain the positive relationship between the occurrence of *C. anthracinus*-type and water conductivity and the positive response to temperatures that is more pronounced at low conductivity. At higher conductivity, and probably higher nutrient levels, lake trophic status would be less dependent on climate, making occurrence of *Chironomus anthracinus*-type possible at low summer temperature provided that soft bottom sediments are sufficiently organic-rich.

As a result, variations in *Chironomus* in fossil records should be primarily interpreted as responses to food availability, which can be controlled by summer temperature changes but also by lake ontogeny, such as natural eutrophication or sediment infilling and watershed development. Similar processes of indirect influences also affect eurybathic psychrostenothermic taxa but in a reverse way through their requirements on oxygenation and cold temperatures. Over time it could generate a warming bias in summer air temperature reconstruction because of natural eutrophication and sediment infilling, which are unfavourable for oxyphilic cold-stenothermic taxa of the profundal zone leading to replacement by taxa more tolerant to organic enrichment such as *Chironomus* and then by typical warm assemblages of ponds, leading to a summer air temperature signal more difficult to separate from other influences (Korhola et al., 2002; Pliikk et al., 2019). Therefore, choosing a clearwater stratified oligotrophic lake with slow sediment accumulation (“slow aging” lake) as study site should be favored with a purpose of summer temperature reconstruction based on subfossil chironomid assemblages (Walker and Cwynar, 2006). If possible, the analysis of fossil chironomids should also be conducted in parallel with analyses of sedimentary organic matter, such as total organic carbon (TOC) and the C/N ratio to have access to independent proxies of lacustrine trophic trajectory.

To summarize, summer air temperatures shape taxa composition of subfossil chironomid assemblages in lake sediment depending mainly on physiological constraints imposed by water temperature and oxygen availability, as well as on consequences on food and microhabitat availability (Cao et al., 2024; Płóciennik et al., 2020; Reuss et al., 2014; Stivrins et al., 2021; Williams et al., 2020). Therefore, the perceived air temperature preferences of chironomid taxa in surface sediment datasets should be understood as realized or functional summer air temperature preferences, which are incorporating larvae physiology and functional trends from indirect influences. For instance, *Chironomus anthracinus*-type while being physiologically eurytherm appears overall functionally thermophilic in our data. Because of these complex species-environment relationships and multiple possible indirect influential pathways of summer temperatures on chironomids, the validity of the empirical relationship apparent in surface sediment datasets for space-for-time reconstruction relies on summer temperature variations as being the major driving force of lake ecosystem dynamic and then of taxonomic turnover through time. This implies interpreting fossil chironomid assemblage changes before applying a transfer function, by considering taxa autoecology within a holistic view about lake ecosystem changes and their potential drivers (Ilyashuk et al., 2005; Millet et al., 2003). This should ensure the quality of the paleotemperature signal and that it

is not the result of confounding influences from independent local factors (Velle et al., 2010, 2012). Selecting an appropriate study site at the beginning of an investigation is also a crucial step, as it directly affects the likelihood and magnitude of potential confounding factors.

4.4. Accuracy of chironomid-based mean summer air temperature inference models

Overall, our results confirm that subfossil chironomids can be reliable summer paleotemperature proxies (Brooks et al., 2012). Indeed, subfossil chironomid assemblages demonstrated a great ability to provide accurate temperature inferences both using cross-validation of inference models and independent testing on downcore data compared with meteorological measurement. This highlights their high sensitivity to temperature variations, which combined with their short life cycle and great dispersal capacity (Krosch et al., 2011) yield the possibility of high temporal resolution reconstructions and hence, the detection of short paleoclimatic events (Axford et al., 2009; Cwynar and Levesque, 1995; Porinchu et al., 2019).

WA-based reconstructions are originally derived from the species packing model (ter Braak and Barendregt, 1986) based on the idea that species evolve to occupy maximally separated niches with unimodal response curves along the gradient having minimum overlap. Hence, weighting average of environmental values for each taxon should be equally spaced, meaning that WA performs well when taxa are evenly distributed with a good turnover (Birks, 1995). The choice of a WA-based method for our transfer function is appropriate because there is a high taxonomic turnover along the climatic gradient of our training-set and most taxa could be considered to have unimodal response curves to temperature. For taxa displaying rather a monotonical shape with a plateau, we still assumed a unimodal response provided that a broader temperature gradient was sampled, as in the study of Rossaro (1991) in rivers where the 30 °C gradient sampled provided mostly asymmetrical unimodal responses. This asymmetrical structure leads to underestimation and overestimation of temperature optima estimated by simple weighting average and especially for taxa with cut curves on gradient edges. However, the WAPLS by using the residual structure for improving the overall fit of the model partially compensates for these biases of taxa optima and therefore limits the extent of the so-called “edge-effect” (ter Braak and Juggins, 1993), evidenced by higher residuals at both ends of the gradient in cross-validations. The temperature response curves also highlight varied tolerances among taxa, underscoring the significance of this metric in inference calculations. Indeed, the occurrence of taxa with narrow tolerances provides more informative climate insights than abundant taxa with broader tolerances. This justifies the approach used by the fxTWAPLS of weighting the abundances by tolerances in inference calculations.

Combining tolerance weighting and frequency correction, fxTWAPLS slightly outperforms classical WAPLS in cross-validation, probably by using more ecological information and by tackling another bias inherent to weighting averaging calculations in unequal sampling design. The performances are especially enhanced on the colder half of the gradient where sampling frequency is lower (Supp Fig. S4). This suggests a compression bias in WAPLS to the most frequent temperatures of the calibration dataset around 15–17 °C, supported also by fxTWAPLS cross-validated model’s regression slope closer to 1 that would indicate less compression bias (Liu et al., 2020). The reduced compression bias of fxTWAPLS is particularly evident with inferences from the record of Lake Igaliku where the WAPLS systematically overestimated the temperature while fxTWAPLS provided more-accurate inferences with an overall error lower than the 9999-Bootstrap cross-validated RMSEP of the inference model. For Lake Croche there are few differences between both methods because the climatic position of this site is well-sampled in the calibration dataset and does not suffer of compression bias of WAPLS. These cross-validation and independent

testing results on weather data time series demonstrate that the fxTWAPLS performs at least as well as the WAPLS, and even better when moving away from the center and the most frequent values of the calibration temperature gradient. We also note that for the fxTWAPLS reconstruction of Lake Igaliku that the bootstrapped sample specific error (sse) is more variable than with WAPLS. This could be an effect of considering taxa tolerances into the calculation of inferences. We think this higher variability of inference uncertainty with fxTWAPLS is more informative than the near-constant sse produced by classical WAPLS, as it offers more nuanced confidence in the inferred values across samples.

The calibration dataset of this study combined with the fxTWAPLS method with two components provides a new summer temperature transfer function based on subfossil chironomids with cross-validated performances equivalent to others of similar extended temperature gradients already published for the Holarctic region (Table 4). So far, it is the chironomid-based transfer function with the largest temperature gradient and the lowest RMSEP in percent of the total gradient in the Holarctic. The successful applications on testing against weather measurements in both the temperate Laurentian Mountains and in the Arctic of southwestern Greenland suggest a good versatility of this transfer function, which can be used over a wide climatic range in the north-eastern Nearctic region. Application in western Nearctic could also be attempted as it would provide a larger temperature gradient on the warm side for study sites suffering an edge-effect and a lack of modern analogs during past warm periods, as observed by Lemmen and Lacourse (2018) on a record from a coastal lowland lake of southeastern British-Columbia.

Chironomid-inferred temperatures were significantly correlated with meteorological measurements only at Lake Igaliku and not for Lake Croche despite a small absolute temperature difference. This underscores the robust performance of the inference model; however, it demonstrates also that the good statistical performance of an inference model only is not enough for providing a meaningful and informative reconstruction from a fossil record. One of the assumptions of quantitative paleoecology is the existence of a major control of the variable of interest over subfossil assemblages and negligible influences from other variables (Birks et al., 2010; Birks, 1995). Indeed, Hohmann et al. (2023) on dinocyst assemblages in marine sediment cores have shown that only the reconstruction of the primary driver of assemblages within a particular record could provide a significant and meaningful reconstruction about past sea-surface conditions. The same rule should apply for chironomids and temperature reconstruction. At Lake Igaliku, the significant correlation between PC1 assemblage scores and measured temperatures confirms an effective temperature control over assemblages, resulting in an informative reconstruction correlated with measured data. Conversely, the lack of correlation between PC1 scores and weather data at Lake Croche suggests that temperature changes were not enough to drive assemblage variability. As a result, the reconstruction is uninformative, reflecting background noise rather than meaningful temperature trends, despite the high performance of the inference model and its close agreement with observed data. This disparity in temperature sensitivity between Lake Igaliku and Lake Croche suggests varying degrees of vulnerability and resilience to

climate change. While lake size and depth can influence sensitivity, both lakes in our study are large and oligotrophic (in the pre-disturbance state for the Lake Igaliku). Given these similarities, the observed differences are more likely driven by their contrasting temperate and Arctic climate settings, which shape ecological responses differently. This supports the idea that Arctic lakes like Lake Igaliku may be more vulnerable to temperature changes, while temperate lakes like Lake Croche may exhibit greater resilience under similar climatic variations. This underscores the importance of considering lake characteristics when selecting study sites for temperature reconstructions and interpreting inferred variations correctly.

The comparison of PC1 scores with weather station temperatures (Fig. 8) suggests they serve as a good diagnostic of the primary factor controlling of assemblage variability. This approach could help in ecologically interpreting fossil record assemblage changes and verify climate signal within compositional data. Visual comparisons of indicator groups spectrum from Lake Igaliku and Lake Croche (Fig. 8) to the one of the full training-set (Fig. 2) position correctly both lakes along the climatic gradient. As a result, a combined visual comparison of PC1 scores with indicator group spectrum could serve as an initial ecological interpretation of fossil assemblage changes and verify the presence of a climatic signal. Comparison with trends of the Hill's N2 could also be performed as summer temperature is significantly correlated to this metric (Fig. 2).

4.5. Quality of postglacial summer temperature reconstructions at Lake Mista

The fossil record of Lake Mista is in good agreement with PC1 scores, Hill's N2 variations and changes within the spectrum of indicator taxa, suggesting an overriding control of chironomid assemblage variability by climatic changes during the postglacial period (Fig. 10). Therefore, it is relevant to attempt quantitative reconstruction of past summer temperatures at this site.

The three models provide temperature curves with a common pattern of climatic trends broadly corresponding to initial warming after glacier retreat, a warm Mid-Holocene (7000 BP to 4200 BP) and Neoglacial cooling in the Late Holocene (last 4200 years BP). However, they differ substantially in inferred temperatures. Extending the temperature gradient of the calibration dataset with more lakes allowed a better representation of rare taxa. The original reconstruction of Feussom Tcheumeleu et al. (2023) the eastern Canadian transfer function that comprises 79 taxa (Bajolle et al., 2018; Laroque, 2008) while our new calibration dataset includes 100 taxa, including more warm indicators that are also present within the fossil record such as *Labrundinia* and *Pseudochironomus*. Also, the extended temperature gradient on the warm side probably allowed for better estimation of temperature optima of warm indicators already present in the previous 75-lake training-set (i.e. *Polypedium nubeculosum*-type, *Cladopelma lateralis*-type, *Glyptotendipes pallens*-type ...). This resulted in better analogs and improved the goodness-of-fit to temperature of the record (Fig. 11), resulting in a better ability to capture the climatic signal represented by variations within compositional data. With the new calibration dataset, the

Table 4

Bootstrapped cross-validated performances of some chironomid-based transfer functions of the Holarctic region (% gradient is the RMSEP relatively to the total temperature range covered by the transfer function; best parameter values are marked in bold).

Publication	Region	n lakes	variable	range	function	R ²	RMSEP	% gradient
This study	New England/Eastern Canada	182 lakes	JJA	20.9 °C	WAPLS	0.88	1.73 °C	8.28 %
This study	New England/Eastern Canada	182 lakes	JJA	20.9 °C	fxTWAPLS	0.91	1.61 °C	7.70 %
Heiri et al. (2011)	Norway/Switzerland	274 lakes	July	14.9 °C	WAPLS	0.87	1.4 °C	9.40 %
Kotrys et al. (2020)	Norway/Switzerland/Poland	357 lakes	July	16.5 °C	WAPLS	0.91	1.39 °C	8.42 %
Nazarova et al. (2015)	Northern Russia	193 lakes	July	17 °C	WAPLS	0.87	1.35 °C	7.94 %
Medeiros et al. (2022)	Canadian Arctic/Greenland/Iceland/Svalbard	402 lakes	JJA	12 °C	WAPLS	0.72	1.48 °C	12.3 %
Fortin et al. (2015)	Canada/Alaska	485 lakes	July/August	16 °C	WAPLS	0.73	1.8 °C	11.25 %
Bajolle et al. (2018)	Eastern Canada	75 lakes	August	18 °C	WAPLS	0.85	1.67 °C	9.28 %

mid-Holocene thermal maximum (Renssen et al., 2012) is more clearly defined, with inferred temperature 2 °C higher than in the 75-lake training-set. It is also the case for the warm episode of 2500-2000 BP, possibly related to the Roman Warm Period (Holmquist et al., 2016; Solignac et al., 2011, Fig. 12). These differences are even more pronounced when using the fxTWAPLS, reinforcing that this inference technique enables the reconstruction of a broader range of climatic values from a single study site compared to the classical WAPLS (Liu et al., 2020).

The transfer function, based on the new training set and the fxTWAPLS method, yields the most reliable of the three reconstructions at the Lake Mista. It is the only approach that successfully captures colder-than-today events both at the beginning of the postglacial period and during the Late Holocene, notably over the well-documented Little Ice Age (Gennaretti et al., 2014; Miller et al., 2012). It also accurately reflects the warmer-than-today mid-Holocene and the subsequent Neoglacial cooling driven by insolation trends. The cooler early postglacial conditions align with the influence of the nearby Laurentide Ice Sheet at that time (Carcaillet and Richard, 2000; Hausmann et al., 2011). Detecting the Little Ice Age is expected, given supporting proxy evidence from other sites within the broad region of the Gulf of St. Lawrence (Perrier et al., 2022; Wu et al., 2021). These results further confirm that the fxTWAPLS method of Liu et al. (2020) is a reliable method for paleoclimatic reconstructions and that it can even improve them over the traditional WAPLS.

5. Conclusions

In this study, we explored the relationship between summer temperatures and subfossil chironomid assemblages in lake sediments, and how to use it to infer quantitative paleoclimate reconstruction. Through joint analyses of compositional and environmental data, we have demonstrated the complex interplay between chironomids and mean JJA air temperature, unraveling both direct physiological responses and indirect influences mediated by temperature-driven changes in lake functioning. Our findings underscore the importance of considering taxon ecology and lake characteristics for correctly interpreting compositional changes along sediment cores. It also emphasizes the importance of choosing an appropriate study site for minimizing the risk of interferences with confounding variables. A clearwater oligotrophic stratified lake in a watershed relatively stable in vegetation cover and land use on the interest period would be an “ideal” target for guiding study site selection.

Our quantitative reconstructions showed the effectiveness of a training-set with more taxa described over a longer gradient range, combined with a less biased inference technique, in producing robust temperature estimates. The ability of fxTWAPLS to mitigate the compression bias of classical WAPLS paves the way for its widespread application with subfossil chironomids. Concerns may remain about uncertainty quantification of this deterministic method, which is likely to become a growing issue as new reconstructions are produced within multi-site and multi-proxy syntheses. Comparison with probabilistic approaches that properly account for the uncertainty in inferences such as Bayesian modelling could be a future prospect.

The transfer function developed in this paper represents a new operational tool available for generating high-quality paleoclimatic reconstructions based on a widespread and abundant proxy in lake sediments, with potential applications extending from the northern temperate zone to the high latitudes of the Nearctic region.

CRediT authorship contribution statement

Thomas Suranyi: Conceptualization, Methodology, Software, Validation, Formal analysis, Investigation, Data curation, Writing – original draft, Visualization, Project administration. **Julie Talbot:** Writing – original draft, Supervision, Project administration. **Donna Francis:**

Validation, Investigation, Data curation, Writing – review & editing. **Augustin Feussom Tcheumeleu:** Validation, Investigation, Data curation, Writing – review & editing. **Pierre Grondin:** Writing – review & editing, Project administration, Funding acquisition. **Damien Rius:** Conceptualization, Investigation, Writing – review & editing. **Adam A. Ali:** Writing – review & editing, Funding acquisition. **Yves Bergeron:** Writing – review & editing, Funding acquisition. **Laurent Millet:** Conceptualization, Methodology, Validation, Investigation, Writing – original draft, Supervision, Project administration, Funding acquisition.

Data availability

The dataset supporting the transfer function of this study has been archived in the Mendeley Data repository (<https://doi.org/10.17632/5jdkzyfw9p.1>). A R script for a shiny app (PaleoRecon Dashboard) is also provided in the repository, allowing users to reproduce cross-validation, reconstruction and diagnostics results of the paper.

Declaration of competing interest

The authors declare that they have no known competing financial interests or personal relationships that could have appeared to influence the work reported in this paper.

Acknowledgements

This research was supported by a MITACS-acceleration PhD grant for the project “Dynamique forestière contemporaine et passée des érablières Nordiques” in partnership with Forex Inc., the CNRS-INSU structuring initiative EC2CO (project “CHAZAM”), and the International Research Project “Cold Forests”. We are grateful to Arthur Millet, Alexandra Millet, Hélène Masclaux, Natasha Roy, Reinhard Pienitz, Camille Latourelle Vigeant, Jonathan Lesven, Milva Druguet-Dayras, Marie-Pier Ménard, Mathilde Bélair, Jessyca Guénette, Médéric Durand, and Jordan Paillard for their invaluable assistance with field sampling. We acknowledge the logistical support provided by Sépaq, IRL Forêt froides, FERLD (Forêt d’enseignement et de recherche du lac Duparquet), and the Station de biologie des Laurentides during the field campaigns. Special thanks go to Jean-François Lapierre for his support with limnological analysis equipment, and to Pierre Legendre for his teaching during his course on quantitative multivariate data analysis, which inspired this work. We also thank Olivier Blarquez for his initial guidance at the beginning of the project. We thank the reviewers for their constructive comments, which have helped improve the quality of our manuscript.

Appendix. A Supplementary data

Supplementary data to this article can be found online at <https://doi.org/10.1016/j.quascirev.2025.109333>.

Data availability

A link to the data and/or code is provided as part of this submission.

References

- Aagaard, K., 1986. The chironomid fauna of north Norwegian lakes, with a discussion on methods of community classification. *Holarctic Ecology* 9, 1–12.
- Appleby, P.G., Oldfield, F., 1978. The calculation of lead-210 dates assuming a constant rate of supply of unsupported 210Pb to the sediment. *Catena* 5, 1–8. [https://doi.org/10.1016/S0341-8162\(78\)80002-2](https://doi.org/10.1016/S0341-8162(78)80002-2).
- Axford, Y., Briner, J.P., Francis, D.R., Miller, G.H., Walker, I.R., Wolfe, A.P., 2011. Chironomids record terrestrial temperature changes throughout Arctic interglacials of the past 200,000 yr. *Bull. Geol. Soc. Am.* 123 (1), 1275–1287. <https://doi.org/10.1130/B30329>.

- Axford, Y., Briner, J.P., Miller, G.H., Francis, D.R., 2009. Paleocological evidence for abrupt cold reversals during peak Holocene warmth on Baffin Island, Arctic Canada. *Quat Res* 71, 142–149. <https://doi.org/10.1016/j.yqres.2008.09.006>.
- Bajolle, L., Larocque-Tobler, I., Gandouin, E., Lavoie, M., Bergeron, Y., Ali, A.A., 2018. Major postglacial summer temperature changes in the central coniferous boreal forest of Quebec (Canada) inferred using chironomid assemblages. *J. Quat. Sci.* 33, 409–420. <https://doi.org/10.1002/jqs.3022>.
- Bakumenko, V., Poska, A., Plóciennik, M., Gasteviciene, N., Kotrys, B., Luoto, T.P., Belle, S., Veski, S., 2024. Chironomidae-based inference model for mean July air temperature reconstructions in the eastern Baltic area. *Boreas*. <https://doi.org/10.1111/bor.12655>.
- Balci, P., Kennedy, J.H., 2002. Secondary production of apedilum elachistum townes (Diptera: Chironomidae) in simulated reservoir wetlands. *Wetlands* 22, 669–676. [https://doi.org/10.1672/0277-5212\(2002\)022\[0669:SPOAET\]2.0.CO;2](https://doi.org/10.1672/0277-5212(2002)022[0669:SPOAET]2.0.CO;2).
- Barley, E.M., Walker, I.R., Kurek, J., Cwynar, L.C., Mathewes, R.W., Gajewski, K., Finney, B.P., 2006. A northwest North American training set: distribution of freshwater midges in relation to air temperature and lake depth. *J. Paleolimnol.* 36, 295–314. <https://doi.org/10.1007/s10933-006-0014-6>.
- Belle, S., Millet, L., Verneaux, V., Lami, A., David, E., Murgia, L., Parent, C., Musazzi, S., Gauthier, E., Bichet, V., Magny, M., 2016. 20Th century human pressures drive reductions in deepwater oxygen leading to losses of benthic methane-based food webs. *Quat. Sci. Rev.* 137, 209–220. <https://doi.org/10.1016/j.quascirev.2016.02.019>.
- Belle, S., Verneaux, V., Mariet, A.L., Millet, L., 2017. Impact of eutrophication on the carbon stable-isotopic baseline of benthic invertebrates in two deep soft-water lakes. *Freshw. Biol.* 62, 1105–1115. <https://doi.org/10.1111/fwb.12931>.
- Bennett, K.D., 1996. Determination of the number of zones in a biostratigraphical sequence. *New Phytol.* 132 (1), 155–170. <https://doi.org/10.1111/j.14698137.1996.tb04521.x>.
- Bilyj, B., Davies, L.J., 1989. Descriptions and ecological notes on seven new species of Cladotanytarsus (Chironomidae: Diptera) collected from an experimentally acidified lake. *Can. J. Zool.* 67, 948–962. <https://doi.org/10.1139/z89-138>.
- Birks, H.J.B., Heiri, O., Seppä, H., Bjune, A.E., 2010. Strengths and weaknesses of quantitative climate reconstructions based on late-quaternary biological proxies. *Open Ecol. J.* 3, 68–110. <https://doi.org/10.2174/1874213001003020068>.
- Birks, J.B., 1995. Quantitative palaeoenvironmental reconstructions. In: Maddy, D., Brew, J.S. (Eds.), *Statistical Modelling of Quaternary Science Data*. Quaternary Research Association, Cambridge, pp. 161–254.
- Blaauw, M., Christen, J.A., 2011. Flexible paleoclimate age-depth models using an autoregressive gamma process. *Bayesian Anal.* 6. <https://doi.org/10.1214/11-BA618>.
- Blarquez, O., Ali, A.A., Girardin, M.P., Grondin, P., Fréchette, B., Bergeron, Y., Hély, C., 2015. Regional paleofire regimes affected by non-uniform climate, vegetation and human drivers. *Sci. Rep.* 5, 13356. <https://doi.org/10.1038/srep13356>.
- Bolland, A., Kern, O.A., Koutsodendrakis, A., Pross, J., Heiri, O., 2022. Chironomid-inferred summer temperature development during the late Rissian glacial, Eemian interglacial and earliest Würmian glacial at Fūramoos, southern Germany. *Boreas* 51, 496–516. <https://doi.org/10.1111/bor.12567>.
- Borcard, D., Legendre, P., Drapeau, P., 1992. Partialling out the spatial component of ecological variation. *Ecology* 73, 1045–1055.
- Borcard, D., Gillet, F., Legendre, P., 2018. *Numerical Ecology with R*, second ed. Springer. <https://doi.org/10.1007/978-3-319-71404-2>.
- Brinkhurst, R.O., 1974. *The Benthos of Lakes*. Macmillan Education UK, London. <https://doi.org/10.1007/978-1-349-15556-9>.
- Brodersen, K.P., Anderson, N.J., 2002. Distribution of chironomids (Diptera) in low arctic West Greenland lakes: trophic conditions, temperature and environmental reconstruction. *Freshw. Biol.* 47, 1137–1157. <https://doi.org/10.1046/j.1365-2427.2002.00831.x>.
- Brodersen, K.P., Pedersen, O., Walker, I.R., Jensen, M.T., 2008. Respiration of midges (Diptera: Chironomidae) in British Columbian lakes: oxy-regulation, temperature and their role as palaeo-indicators. *Freshw. Biol.* 53, 593–602. <https://doi.org/10.1111/j.1365-2427.2007.01922.x>.
- Brooks, S.J., 2000. Lateglacial fossil midge (insecta: Diptera: Chironomidae) stratigraphies from the Swiss alps. *Palaeogeogr. Palaeoclimatol. Palaeoecol.* 159, 261–279.
- Brooks, S.J., Axford, Y., Heiri, O., Langdon, P.G., Larocque-Tobler, I., 2012. Chironomids can be reliable proxies for Holocene temperatures. A comment on Velle et al. (2010). *Holocene* 22, 1495–1500. <https://doi.org/10.1177/0959683612449757>.
- Brooks, S.J., Birks, H.J.B., 2001. Chironomid-inferred air temperatures from Lateglacial and Holocene sites in north-west Europe: progress and problems. *Quat. Sci. Rev.* 20, 1723–1741. [https://doi.org/10.1016/S0277-3791\(01\)00038-5](https://doi.org/10.1016/S0277-3791(01)00038-5).
- Brooks, S.J., Langdon, P.G., Heiri, O., 2007. In: *The Identification and Use of Palaeo-archaic Chironomidae Larvae in Palaeoecology*, QRA Techni. London.
- Brundin, L., 1958. The bottom faunistic lake-type system. *Int. Ver. Theor. Angew. Limnol. Verh.* 13, 288–297.
- Brundin, L., 1956. Die bodenfaunistischen Seetypen und ihre Anwendbarkeit auf die Südhalfkugel. Zugleich eine Theorie der produktionsbiologischen Bedeutung der glazialen Erosion. *Rep. Inst. Freshw. Res. Drottningholm* 37, 186–235.
- Brundin, L., 1949. Chironomiden und andere Bodentiere der Südschwedischen Urbergseen. Ein Beitrag zur Kenntnis der bodenfaunistischen Charakterzüge Schwedischer oligotropher Seen. *Drottningholm*.
- Cáceres, M.D., Legendre, P., 2009. Associations between species and groups of sites: Indices and statistical inference. *Ecology* 90 (12), 3566–3574. R package version 1.7.12. Available at: <https://CRAN.R-project.org/package=indicspecies>.
- Cao, Y., Langdon, P.G., Shen, S., Li, H., Pan, D., 2024. Using functional traits of chironomids to determine habitat changes in subtropical wetlands. *Ecol. Indic.* 159, 111656. <https://doi.org/10.1016/j.ecolind.2024.111656>.
- Cao, Y., Langdon, P.G., Yan, Y., Wang, S., Zheng, Z., Zhang, Z., 2019. Chironomid communities from subalpine peatlands in subtropical China as indicators of environmental change. *J. Paleolimnol.* 62, 165–179. <https://doi.org/10.1007/s10933-019-00081-5>.
- Carcaillet, C., Richard, P.J.H., 2000. Holocene changes in seasonal precipitation highlighted by fire incidence in eastern Canada. *Clim. Dyn.* 16, 549–559. <https://doi.org/10.1007/s003820000062>.
- Chang, W., Cheng, J., Allaire, J., Sievert, C., Schloerke, B., Xie, Y., Allen, J., McPherson, J., Dipert, A., Borges, B., 2024. shiny: Web Application Framework for R. R package. <https://doi.org/10.32614/CRAN.package.shiny>, version 1.10.0.
- Cwynar, L.C., Levesque, A.J., 1995. Chironomid evidence for late-glacial climatic reversals in Maine. *Quaternary Research* 43, 405–413. <https://doi.org/10.1006/qres.1995.1046>.
- Da Silva, F.L., Fonseca-Gessner, A.A., Ekrem, T., 2014. A taxonomic revision of genus *Labrundinia* fittkau, 1962 (Diptera: Chironomidae: Tanypodinae). *Zootaxa* 3769, 1–185. <https://doi.org/10.11646/zootaxa.3769.1.1>.
- De'ath, G., 2002. Multivariate regression trees: a new technique for modeling species-environment relationships. *Ecology* 83, 1105–1117. [https://doi.org/10.1890/0012-9658\(2002\)083\[1105:MRTANT\]2.0.CO;2](https://doi.org/10.1890/0012-9658(2002)083[1105:MRTANT]2.0.CO;2).
- De'ath, G., 2007. mvpart: multivariate partitioning. R package version 1, 6-2. Available at: <https://CRAN.R-project.org/package=mvpart>.
- Dickson, T.R., Walker, I.R., 2015. Midge (Diptera: Chironomidae and Ceratopogonidae) emergence responses to temperature: experiments to assess midges' capacity as paleotemperature indicators. *J. Paleolimnol.* 53, 165–176. <https://doi.org/10.1007/s10933-014-9814-2>.
- Dranga, S.A., Hayles, S., Gajewski, K., 2018. Synthesis of limnological data from lakes and ponds across Arctic and Boreal Canada. *Arct Sci* 4, 167–185. <https://doi.org/10.1139/as-2017-0039>.
- Dufrene, M., Legendre, P., 1997. Species assemblages and indicator species: the need for a flexible asymmetrical approach. *Ecol. Monogr.* 67, 345. <https://doi.org/10.2307/2963459>.
- Eggermont, H., Heiri, O., 2012. The chironomid-temperature relationship: Expression in nature and palaeoenvironmental implications. *Biol. Rev.* 87, 430–456. <https://doi.org/10.1111/j.1469-185X.2011.00206.x>.
- Eggermont, H., Heiri, O., Russell, J., Vuille, M., Audenaert, L., Verschuren, D., 2010. Paleotemperature reconstruction in tropical Africa using fossil Chironomidae (insecta: Diptera). *J. Paleolimnol.* 43, 413–435. <https://doi.org/10.1007/s10933-009-9339-2>.
- Engels, S., Medeiros, A.S., Axford, Y., Brooks, S.J., Heiri, O., Luoto, T.P., Nazarova, L., Porinchi, D.F., Quinlan, R., Self, A.E., 2020. Temperature change as a driver of spatial patterns and long-term trends in chironomid (Insecta: Diptera) diversity. *Glob Chang Biol* 26, 1155–1169. <https://doi.org/10.1111/gcb.14862>.
- Epler, J.H., 2001. *Identification Manual for the Larval Chironomidae (Diptera) of North and South Carolina. A Guide to the Taxonomy of the Midges of the Southeastern United States, Including Florida*.
- Feussom Tcheumeleu, A., Millet, L., Rius, D., Ali, A.A., Bergeron, Y., Grondin, P., Gauthier, S., Blarquez, O., 2023. An 8500-year history of climate-fire-vegetation interactions in the eastern maritime black spruce-moss bioclimatic domain, Québec, Canada. *Ecoscience* 1–17. <https://doi.org/10.1080/11956860.2023.2292354>.
- Fick, S.E., Hijmans, R.J., 2017. WorldClim 2: new 1-km spatial resolution climate surfaces for global land areas. *Int. J. Climatol.* 37, 4302–4315. <https://doi.org/10.1002/joc.5086>.
- Fortin, M.-C., Medeiros, A.S., Gajewski, K., Barley, E.M., Larocque-Tobler, I., Porinchi, D.F., Wilson, S.E., 2015. Chironomid-environment relations in northern North America. *J. Paleolimnol.* 54, 223–237. <https://doi.org/10.1007/s10933-015-9848-0>.
- Francis, D.R., 2004. Distribution of midge remains (Diptera: Chironomidae) in surficial lake sediments in New England. *Northeast. Nat.* 11, 459–478. [https://doi.org/10.1656/1092-6194\(2004\)011\[0459:DOMRDC\]2.0.CO;2](https://doi.org/10.1656/1092-6194(2004)011[0459:DOMRDC]2.0.CO;2).
- Francis, D.R., Wolfe, A.P., Walker, I.R., Miller, G.H., 2006. Interglacial and Holocene temperature reconstructions based on midge remains in sediments of two lakes from Baffin Island, Nunavut, Arctic Canada. *Palaeogeogr. Palaeoclimatol. Palaeoecol.* 236, 107–124. <https://doi.org/10.1016/j.palaeo.2006.01.005>.
- Frossard, V., Millet, L., Verneaux, V., Jenny, J.P., Arnaud, F., Magny, M., Poulencard, J., Perga, M.E., 2013. Chironomid assemblages in cores from multiple water depths reflect oxygen-driven changes in a deep French lake over the last 150 years. *J. Paleolimnol.* 50, 257–273. <https://doi.org/10.1007/s10933-013-9722-x>.
- Gennaretti, F., Arseneault, D., Nicault, A., Perreault, L., Begin, Y., 2014. Volcano-induced Regime Shifts in Millennial Tree-Ring Chronologies from Northeastern North America, vol. 111. *Proceedings of the National Academy of Sciences*, pp. 10077–10082. <https://doi.org/10.1073/pnas.1324220111>.
- Gerstmeier, R., 1989. Phenology and bathymetric distribution of the profundal chironomid fauna in Starnberger See (F.R. Germany) - Diptera, Chironomidae. *Hydrobiologia* 184, 29–42. <https://doi.org/10.1007/BF00014299>.
- Girardin, M.P., Gaboriau, D.M., Ali, A.A., Gajewski, K., Briere, M.D., Bergeron, Y., Paillard, J., Waito, J., Tardif, J.C., 2024. Boreal forest cover was reduced in the mid-Holocene with warming and recurring wildfires. *Commun Earth Environ* 5. <https://doi.org/10.1038/s43247-024-01340-8>.
- Griffiths, K., Jeziorski, A., Antoniadis, D., Smol, J.P., Gregory-Eaves, I., 2024. Changes in midge assemblages reflect climate and trophic gradients across north temperate and boreal lakes since the pre-industrial period. *Freshw. Biol.* 69, 15–33. <https://doi.org/10.1111/fwb.14189>.

- Grimm, E.C., 1987. CONISS: a FORTRAN 77 program for stratigraphically constrained cluster analysis by the method of incremental sum of squares. *Comput. Geosci.* 13 (1), 13–35. [https://doi.org/10.1016/0098-3004\(87\)90022-7](https://doi.org/10.1016/0098-3004(87)90022-7).
- Hamerlík, L., Svitok, M., Novíkvec, M., Veselská, M., Bitušák, P., 2017. Weak altitudinal pattern of overall chironomid richness is a result of contrasting trends of subfamilies in high-altitude ponds. *Hydrobiologia* 793, 67–81. <https://doi.org/10.1007/s10750-016-2992-3>.
- Hausmann, S., Larocque-Tobler, I., Richard, P.J.H., Pienitz, R., St-Onge, G., Fye, F., 2011. Diatom-inferred wind activity at Lac du sommet, southern Québec, Canada: A multiproxy paleoclimate reconstruction based on diatoms, chironomids and pollen for the past 9500 years. *Holocene* 21, 925–938. <https://doi.org/10.1177/0959683611400199>.
- Heiri, O., 2001. *Holocene palaeolimnology of Swiss mountain lakes reconstructed using subfossil chironomid remains. Past Climate and Prehistoric Human Impact on Lake Ecosystems (PhD Thesis)*. University of Bern.
- Heiri, O., Brooks, S.J., Birks, H.J.B., Lotter, A.F., 2011. A 274-lake calibration data-set and inference model for chironomid-based summer air temperature reconstruction in Europe. *Quat. Sci. Rev.* 30, 3445–3456. <https://doi.org/10.1016/j.quascirev.2011.09.006>.
- Helwig, N.E., 2024. npreg: Nonparametric Regression via Smoothing Splines. R package version 1.1-0. Available at: <https://CRAN.R-project.org/package=npreg>.
- Hofmann, W., 1988. The significance of chironomid analysis (Insecta: Diptera) for paleolimnological research. *Palaeogeogr. Palaeoclimatol. Palaeoecol.* 62, 501–509. [https://doi.org/10.1016/0031-0182\(88\)90070-3](https://doi.org/10.1016/0031-0182(88)90070-3).
- Hofmann, W., 1971. Die postglaziale Entwicklung der Chironomiden- und Chaoborus-Fauna (Dipt.) des Schösee. *Arch. Hydrobiol.* 40 (1), 74.
- Hohmann, S., Kucera, M., De Vernal, A., 2023. Disentangling environmental drivers of subarctic dinocyst assemblage compositional change during the Holocene. *Clim. Past* 19, 2027–2051. <https://doi.org/10.5194/cp-19-2027-2023>.
- Holmes, N., Langdon, P.G., Caseldine, C., Brooks, S.J., Birks, H.J.B., 2011. Merging chironomid training sets: implications for palaeoclimate reconstructions. *Quat. Sci. Rev.* 30, 2793–2804. <https://doi.org/10.1016/j.quascirev.2011.06.013>.
- Holmquist, J.R., Booth, R.K., MacDonald, G.M., 2016. Boreal peatland water table depth and carbon accumulation during the Holocene thermal maximum, Roman Warm Period, and Medieval Climate Anomaly. *Palaeogeogr. Palaeoclimatol. Palaeoecol.* 444, 15–27. <https://doi.org/10.1016/j.palaeo.2015.11.035>.
- Hutchinson, G.E., 1957. Concluding remarks. *Cold Spring Harb Symp Quant Biol* 22, 415–427. <https://doi.org/10.1101/SQB.1957.022.01.039>.
- Ilyashuk, E.A., Ilyashuk, B.P., Hammarlund, D., Larocque, I., 2005. Holocene climatic and environmental changes inferred from midge records (Diptera: Chironomidae, Chaoboridae, Ceratopogonidae) at Lake Berkut, southern Kola Peninsula, Russia. *Holocene* 15, 897–914. <https://doi.org/10.1191/0959683605hl865ra>.
- Jennings, D.R.H., 2021. Does glacial retreat impact benthic chironomid communities? A case study from Rocky Mountain National Park, Colorado. *SN Appl. Sci.* 3, 855. <https://doi.org/10.1007/s42452-021-04835-7>.
- Juggins, S., 2023. *Rioja: Analysis of Quaternary Science Data*.
- Juggins, S., 2013. Quantitative reconstructions in palaeolimnology: new paradigm or sick science? *Quat. Sci. Rev.* 64, 20–32. <https://doi.org/10.1016/j.quascirev.2012.12.014>.
- Korhola, A., Vasko, K., Toivonen, H.T.T., Olander, H., 2002. Holocene temperature changes in northern Fennoscandia reconstructed from chironomids using Bayesian modelling. *Quat. Sci. Rev.* 21, 1841–1860. [https://doi.org/10.1016/S0277-3791\(02\)00003-3](https://doi.org/10.1016/S0277-3791(02)00003-3).
- Kotrys, B., Plóciennik, M., Sydor, P., Brooks, S.J., 2020. Expanding the Swiss-Norwegian chironomid training set with Polish data. *Boreas* 49, 89–107. <https://doi.org/10.1111/bor.12406>.
- Krosch, M.N., Baker, A.M., Mather, P.B., Cranston, P.S., 2011. Systematics and biogeography of the gondwanan orthoclaadiinae (Diptera: Chironomidae). *Mol. Phylogenet. Evol.* 59, 458–468. <https://doi.org/10.1016/j.ympev.2011.03.003>.
- Larocque, I., 2008. *Nouvelle fonction de transfert pour reconstruire la température à l'aide des chironomides préservés dans les sédiments lacustres*.
- Larocque, I., Grosjean, M., Heiri, O., Bigler, C., Blass, A., 2009. Comparison between chironomid-inferred July temperatures and meteorological data AD 1850–2001 from varved Lake Silvaplana, Switzerland. *J. Paleolimnol.* 41, 329–342. <https://doi.org/10.1007/s10933-008-9228-0>.
- Larocque, I., Hall, R.L., Grahn, E., 2001. Chironomids as indicators of climate change: a 100-lake training set from a subarctic region of northern Sweden (Lapland). *J. Paleolimnol.* 26, 307–322. <https://doi.org/10.1023/A:1017524101783>.
- Larocque, I., Pienitz, R., Rolland, N., 2006. Factors influencing the distribution of chironomids in lakes distributed along a latitudinal gradient in northwestern Quebec, Canada. *Can. J. Fish. Aquat. Sci.* 63, 1286–1297. <https://doi.org/10.1139/f06-020>.
- Larocque-Tobler, I., 2010. Reconstructing temperature at Egelsee, Switzerland, using North American and Swedish chironomid transfer functions: potential and pitfalls. *J. Paleolimnol.* 44, 243–251. <https://doi.org/10.1007/s10933-009-9400-1>.
- Larsen, D.R., Speckman, P.L., 2004. Multivariate regression trees for analysis of abundance data. *Biometrics* 60, 543–549. <https://doi.org/10.1111/j.0006-341X.2004.00202.x>.
- Legendre, P., Gallagher, E.D., 2001. Ecologically meaningful transformations for ordination of species data. *Oecologia* 129, 271–280. <https://doi.org/10.1007/s004420100716>.
- Legendre, P., Legendre, L., 2012. Ecological resemblance. In: Legendre, P., Legendre, L. (Eds.), *Numerical Ecology*. Elsevier Science, Amsterdam, pp. 265–335. <https://doi.org/10.1016/B978-0-444-53868-0.50007-1>.
- Legendre, P., Oksanen, J., ter Braak, C.J.F., 2011. Testing the significance of canonical axes in redundancy analysis. *Methods Ecol. Evol.* 2, 269–277. <https://doi.org/10.1111/j.2041-210X.2010.00078.x>.
- Lehmann, J., Lacourse, T., 2018. Fossil chironomid assemblages and inferred summer temperatures for the past 14,000 years from a low-elevation lake in Pacific Canada. *J. Paleolimnol.* 59, 427–442. <https://doi.org/10.1007/s10933-017-9998-3>.
- Lencioni, V., Bernabò, P., Vanin, S., Di Muro, P., Beltrami, M., 2008. Respiration rate and oxy-regulatory capacity in cold stenothermal chironomids. *J. Insect. Physiol.* 54, 1337–1342. <https://doi.org/10.1016/j.jinsphys.2008.07.002>.
- Lindegaard, C., 1995. Chironomidae (Diptera) of European cold springs and factors influencing their distribution. *Journal of the Kansas Entomological Society* 68, 108–131.
- Liu, M., Prentice, I.C., Ter Braak, C.J.F., Harrison, S.P., 2020. An improved statistical approach for reconstructing past climates from biotic assemblages: improved palaeoclimate reconstruction. *Proc. R. Soc. A* 476. <https://doi.org/10.1098/rspa.2020.0346>.
- Livingstone, D.M., Lotter, F., 1998. The relationship between air and water temperatures in lakes of the Swiss Plateau. *J. Paleolimnol.* 19, 181–198.
- Lods-Crozet, B., Lachavanne, J.B., 1994. Changes in the chironomid communities in Lake Geneva in relation with eutrophication, over a period of 60 years. *Arch. Hydrobiol.* 130, 453–471. <https://doi.org/10.1127/archiv-hydrobiol/130/1994/453>.
- Loskutova, O.A., Kondratjeva, T.A., Nazarova, L.B., 2023. Chironomids of thermal and karst springs of the Bolshezemelskaya tundra. *Aquat. Insects* 1–14. <https://doi.org/10.1080/01650424.2023.2299816>.
- Lotter, A.F., Walker, I.R., Brooks, S.J., Hofmann, W., 1999. An intercontinental comparison of chironomid palaeotemperature inference models: Europe vs North America. *Quat. Sci. Rev.* 18, 717–735. [https://doi.org/10.1016/S0277-3791\(98\)00044-4](https://doi.org/10.1016/S0277-3791(98)00044-4).
- Luoto, T.P., Rantala, M.V., Galkin, A., Rautio, M., Nevalainen, L., 2016. Environmental determinants of chironomid communities in remote northern lakes across the treeline—implications for climate change assessments. *Ecol. Indic.* 61, 991–999. <https://doi.org/10.1016/j.ecolind.2015.10.057>.
- Luoto, T.P., Ojala, A.E.K., 2017. Meteorological validation of chironomids as a palaeotemperature proxy using varved lake sediments. *Holocene* 27, 870–878. <https://doi.org/10.1177/09596836166675940>.
- Luoto, T.P., Ojala, A.E.K., Zajackowski, M., 2019. Proxy-based 300-year high arctic climate warming record from svalbard. *Polar Rec.* 55, 132–141. <https://doi.org/10.1017/S0032247419000275>.
- Magnan, G., Stum-boivin, L.E., Garneau, M., Grondin, P., Fenton, N., Bergeron, Y., 2019. Holocene vegetation dynamics and hydrological variability in forested peatlands of the Clay Belt, eastern Canada, reconstructed using a palaeoecological approach. *Boreas* 48, 131–146. <https://doi.org/10.1111/bor.12345>.
- Matthews-Bird, F., Brooks, S.J., Holden, P.B., Montoya, E., Gosling, W.D., 2016. Inferring late-Holocene climate in the Ecuadorian Andes using a chironomid-based temperature inference model. *Clim. Past* 12, 1263–1280. <https://doi.org/10.5194/cp-12-1263-2016>.
- Mayfield, R.J., Rijal, D.P., Heintzman, P.D., Langdon, P.G., Karger, D.N., Brown, A.G., Alsos, I.G., 2024. Holocene summer temperature reconstruction from plant sedaDNA and chironomids from the northern boreal forest. *Quat. Sci. Rev.* 345, 109045. <https://doi.org/10.1016/j.quascirev.2024.109045>.
- McKeeown, M.M., Caseldine, C.J., Thompson, G., Langdon, P.G., Holmes, N., Brooks, S.J., Rymel, L., 2019. Complexities in interpreting chironomid-based temperature reconstructions over the Holocene from a lake in Western Ireland. *Quat. Sci. Rev.* 222, 105908. <https://doi.org/10.1016/j.quascirev.2019.105908>.
- Medeiros, A.S., Chipman, M.L., Francis, D.R., Hamerlík, L., Langdon, P., Puleo, P.J.K., Schellinger, G., Steigleder, R., Walker, I.R., Woodroffe, S., Axford, Y., 2022. A continental-scale chironomid training set for reconstructing Arctic temperatures. *Quat. Sci. Rev.* 294, 107728. <https://doi.org/10.1016/j.quascirev.2022.107728>.
- Medeiros, A.S., Quinlan, R., 2011. The distribution of the Chironomidae (Insecta: Diptera) along multiple environmental gradients in lakes and ponds of the eastern Canadian Arctic. *Can. J. Fish. Aquat. Sci.* 68, 1511–1527. <https://doi.org/10.1139/f2011-076>.
- Miller, G.H., Geirsdóttir, Á., Zhong, Y., Larsen, D.J., Otto-Bliesner, B.L., Holland, M.M., Bailey, D.A., Refsnyder, K.A., Lehman, S.J., Southon, J.R., Anderson, C., Björnsson, H., Thordarson, T., 2012. Abrupt onset of the Little Ice Age triggered by volcanism and sustained by sea-ice/ocean feedbacks. *Geophys. Res. Lett.* 39. <https://doi.org/10.1029/2011GL050168> n/a-n/a.
- Millet, L., Giguët-Covex, C., Verneaux, V., Druart, J.-C., Adatte, T., Arnaud, F., 2010. Reconstruction of the recent history of a large deep prealpine lake (Lake Bourget, France) using subfossil chironomids, diatoms, and organic matter analysis: towards the definition of a lake-specific reference state. *J. Paleolimnol.* 44, 963–978. <https://doi.org/10.1007/s10933-010-9467-8>.
- Millet, L., Massa, C., Bichet, V., Frossard, V., Belle, S., Gauthier, E., 2014. Anthropogenic versus climatic control in a high-resolution 1500-year chironomid stratigraphy from a southwestern Greenland lake. *Quat. Res.* 81, 193–202. <https://doi.org/10.1016/j.yqres.2014.01.004>.
- Millet, L., Verneaux, V., Magny, M., 2003. Lateglacial palaeoenvironmental reconstruction using subfossil chironomid assemblages from Lake Lautrey (Jura, France). *Arch. Hydrobiol.* 156, 405–429. <https://doi.org/10.1127/0003-9136/2003/0156-0405>.
- Motta, L., Massaferro, J., 2019. Climate and site-specific factors shape chironomid taxonomic and functional diversity patterns in northern Patagonia. *Hydrobiologia* 839, 131–143. <https://doi.org/10.1007/s10750-019-04001-6>.
- Nazarova, L., Self, A.E., Brooks, S.J., van Hardenbroek, M., Herzschuh, U., Diekmann, B., 2015. Northern Russian chironomid-based modern summer temperature data set and inference models. *Glob. Planet. Change* 134, 10–25. <https://doi.org/10.1016/j.gloplacha.2014.11.015>.

- Novikmec, M., Svitok, M., Kočický, D., Šporka, F., Bitušák, P., 2013. Surface water temperature and ice cover of tatra Mountains lakes depend on altitude, topographic shading, and bathymetry. *Arctic Antarct. Alpine Res.* 45, 77–87. <https://doi.org/10.1657/1938-4246-45.1.77>.
- Oliver, D.R., Rousset, M.E., 1983. *The Insects and Arachnids of Canada: Part 11. The Genera of Larval Midges of Canada; Diptera: Chironomidae, the Insects and Arachnids of Canada.* Agriculture Canada Publication, Ottawa.
- Oksanen, J., Blanchet, F.G., Friendly, M., Kindt, R., Legendre, P., McGlinn, D., Minchin, P.R., O'Hara, R.B., Simpson, G.L., Solymos, P., Stevens, M.H.H., Szocs, E., Wagner, H., 2023. *Vegan: community ecology package.* R package version 2, 6-4. Available at: <https://CRAN.R-project.org/package=vegan>.
- Peres-Neto, P.R., Legendre, P., Dray, S., Borcard, D., 2006. Variation partitioning of species data matrices: estimation and comparison of fractions. *Ecology* 87, 2614–2625. [https://doi.org/10.1890/0012-9658\(2006\)87\[2614:VPOSDM\]2.0.CO;2](https://doi.org/10.1890/0012-9658(2006)87[2614:VPOSDM]2.0.CO;2).
- Perrier, L., Sanderson, N.K., Garneau, M., Pratte, S., 2022. Climate-driven Holocene ecohydrological and carbon dynamics from maritime peatlands of the Gulf of St. Lawrence, eastern Canada. *Holocene* 32, 749–763. <https://doi.org/10.1177/09596836221095978>.
- Plikk, A., Engels, S., Luoto, T.P., Nazarova, L., Salonen, J.S., Helmens, K.F., 2019. Chironomid-based temperature reconstruction for the Eemian Interglacial (MIS 5e) at Sokki, northeast Finland. *J. Paleolimnol.* 61, 355–371. <https://doi.org/10.1007/s10933-018-00064-y>.
- Plóciennik, M., Pawlowski, D., Vilizzi, L., Antczak-Orlewska, O., 2020. From oxbow to mire: Chironomidae and Cladocera as habitat palaeoindicators. *Hydrobiologia* 847, 3257–3275. <https://doi.org/10.1007/s10750-020-04327-6>.
- Porinchu, D.F., MacDonald, G.M., Moser, K.A., Rolland, N., Kremenetski, K., Seppä, H., Rühland, K.M., 2019. Evidence of abrupt climate change at 9.3 ka and 8.2 ka in the central Canadian arctic: connection to the north atlantic and atlantic meridional overturning circulation. *Quat. Sci. Rev.* 219, 204–217. <https://doi.org/10.1016/j.quascirev.2019.07.024>.
- Porinchu, D.F., Moser, K.A., Munroe, J.S., 2007. Development of a midge-based summer surface water temperature inference model for the Great Basin of the western United States. *Arctic Antarct. Alpine Res.* 39, 566–577. [https://doi.org/10.1657/1523-0430\(07-033 \[PORINCHU\]\)2.0.CO;2](https://doi.org/10.1657/1523-0430(07-033 [PORINCHU])2.0.CO;2).
- Quinlan, R., Paterson, M.J., Smol, J.P., 2012. Climate-mediated changes in small lakes inferred from midge assemblages: the influence of thermal regime and lake depth. *J. Paleolimnol.* 48, 297–310. <https://doi.org/10.1007/s10933-012-9585-6>.
- Quinlan, R., Smol, J.P., 2001. Chironomid-based inference models for estimating end-of-summer hypolimnetic oxygen from south-central Ontario shield lakes. *Freshw. Biol.* 46, 1529–1551. <https://doi.org/10.1046/j.1365-2427.2001.00763.x>.
- R Core Team, 2022. *R: A Language and Environment for Statistical Computing.* R Foundation for Statistical Computing.
- Rees, A.B.H., Cwynar, L.C., Cranston, P.S., 2008. Midges (Chironomidae, Ceratopogonidae, Chaoboridae) as a temperature proxy: a training set from Tasmania, Australia. *J. Paleolimnol.* 40, 1159–1178. <https://doi.org/10.1007/s10933-008-9222-6>.
- Renssen, H., Seppä, H., Crosta, X., Goosse, H., Roche, D.M., 2012. Global characterization of the holocene thermal maximum. *Quat. Sci. Rev.* 48, 7–19. <https://doi.org/10.1016/j.quascirev.2012.05.022>.
- Reuss, N.S., Hamerlík, L., Velle, G., Michelsen, A., Pedersen, O., Brodersen, K.P., 2014. Microhabitat influence on chironomid community structure and stable isotope signatures in West Greenland lakes. *Hydrobiologia* 730, 59–77. <https://doi.org/10.1007/s10750-014-1821-9>.
- Rigterink, S., Krahn, K.J., Kotrys, B., Urban, B., Heiri, O., Turner, F., Pannes, A., Schwalb, A., 2024. Summer temperatures from the Middle Pleistocene site Schöningen 13 II, northern Germany, determined from subfossil chironomid assemblages. *Boreas*. <https://doi.org/10.1111/bor.12658>.
- Rossaro, B., 1991. Chironomids and water temperature. *Aquat. Insects* 13, 87–98. <https://doi.org/10.1080/01650429109361428>.
- Rossaro, B., Marziali, L., Boggero, A., 2022. Response of chironomids to key environmental factors: Perspective for biomonitoring. *Insects* 13. <https://doi.org/10.3390/insects13100911>.
- Saether, O.A., 1979. Chironomid communities as water quality indicators. *Ecography* 2, 65–74. <https://doi.org/10.1111/j.1600-0587.1979.tb00683.x>.
- Saether, O.A., 1975. Nearctic chironomids as indicators of lake typology. *Verh. Int. Ver. Limnol.* 19, 3127–3133.
- Self, A.E., Brooks, S.J., Birks, H.J.B., Nazarova, L., Porinchu, D., Odland, A., Yang, H., Jones, V.J., 2011. The distribution and abundance of chironomids in high-latitude Eurasian lakes with respect to temperature and continentality: development and application of new chironomid-based climate-inference models in northern Russia. *Quat. Sci. Rev.* 30, 1122–1141. <https://doi.org/10.1016/j.quascirev.2011.01.022>.
- Simpson, G.L., 2007. Analogue methods in palaeoecology: using the analogue package. *J. Stat. Software* 22. <https://doi.org/10.18637/jss.v022.i02>.
- Simpson, G.L., 2018. Modelling palaeoecological time series using generalised additive models. *Front. Ecol. Evol.* 6, 149. <https://doi.org/10.3389/fevo.2018.00149>.
- Solignac, S., Seidenkrantz, M.S., Jessen, C., Kuijpers, A., Gunvald, A.K., Olsen, J., 2011. Late-holocene sea-surface conditions offshore Newfoundland based on dinoflagellate cysts. *Holocene* 21, 539–552. <https://doi.org/10.1177/0959683610385720>.
- Stahl, J.B., 1966. Characteristics of a north American *Sergentia* lake. *Gewässer Abwässer* 41/42, 95–122.
- Stivirins, N., Belle, S., Trasune, L., Blaus, A., Salonen, S., 2021. Food availability and temperature optima shaped functional composition of chironomid assemblages during the Late Glacial–Holocene transition in Northern Europe. *Quat. Sci. Rev.* 266, 107083. <https://doi.org/10.1016/j.quascirev.2021.107083>.
- Telford, R.J., 2018. *ggplot2 Plots for Analogue and Rioja Packages.*
- ter Braak, C.J.F., Juggins, S., 1993. Weighted averaging partial least squares regression (WA-PLS): an improved method for reconstructing environmental variables from species assemblages. *Hydrobiologia* 269–270, 485–502. <https://doi.org/10.1007/BF00028046>.
- ter Braak, C.J.F., Barendregt, L.G., 1986. Weighted averaging of species indicator values: its efficiency in environmental calibration. *Math. Biosci.* 78, 57–72. [https://doi.org/10.1016/0025-5564\(86\)90031-3](https://doi.org/10.1016/0025-5564(86)90031-3).
- Thienemann, A., 1954. *Chironomus: Leben, Verbreitung und wirtschaftliche Bedeutung der Chironomiden*, vol. 20.
- Thienemann, A., 1920. *Untersuchungen über die Beziehungen zwischen dem Sauerstoffgehalt des Wassers und der Zusammensetzung der Fauna in norddeutschen Seen.* *Arch. Hydrobiol.* 12, 1–65.
- U.S. Environmental Protection Agency (EPA), 2016. Level I ecoregions of north America. Retrieved from: <https://www.epa.gov/eco-research/ecoregions-north-america>.
- van Bellen, S. Van, Garneau, M., Booth, R.K., 2011. Holocene carbon accumulation rates from three ombrotrophic peatlands in boreal Quebec, Canada: impact of climate-driven ecohydrological change. *Holocene* 21, 1217–1231. <https://doi.org/10.1177/0959683611405243>.
- van der Voet, H., 1994. Comparing the predictive accuracy of models using a simple randomization test. *Chemometr. Intell. Lab. Syst.* 25, 313–323. [https://doi.org/10.1016/0169-7439\(94\)85050-X](https://doi.org/10.1016/0169-7439(94)85050-X).
- Velle, G., Brodersen, K.P., Birks, H.J.B., Willassen, E., 2012. Inconsistent results should not be overlooked: A reply to Brooks et al. (2012). *Holocene* 22, 1501–1508. <https://doi.org/10.1177/0959683612449765>.
- Velle, G., Brodersen, K.P., Birks, H.J.B., Willassen, E., 2010. Midges as quantitative temperature indicator species: lessons for palaeoecology. *Holocene* 20, 989–1002. <https://doi.org/10.1177/0959683610365933>.
- Walker, Ian R., Levesque, A.J., Cwynar, L.C., Lotter, A.F., 1997. An expanded surface-water palaeotemperature inference model for use with fossil midges from eastern Canada. *J. Paleolimnol.* 18, 165–178.
- Walker, I.R., Cwynar, L.C., 2006. Midges and palaeotemperature reconstruction—the North American experience. *Quat. Sci. Rev.* 25, 1911–1925. <https://doi.org/10.1016/j.quascirev.2006.01.014>.
- Walker, I.R., Fernando, C.H., Paterson, C.G., 1985. Associations of Chironomidae (Diptera) of shallow, acid, humic lakes and bog pools in Atlantic Canada, and a comparison with an earlier paleoecological investigation. *Hydrobiologia* 120, 11–22. <https://doi.org/10.1007/BF00034586>.
- Walker, I.R., Paterson, C.G., 1983. Post-glacial chironomid succession in two small, humic lakes in the new brunswick - nova scotia (Canada) border area. *Freshw. Invertebr. Biol.* 2, 61–73.
- Whittaker, R.H., Levin, S.A., Root, R.B., 1973. Niche, habitat, and ecotone. *Am. Nat.* 107, 321–338.
- Wiederholm, T., 1983. *Chironomidae of the Holarctic region. Keys and diagnoses. Part 1: Larvae.* *Entomologica Scandinavica Suppl.* 19, 1–457.
- Williams, N., Suárez, D.A., Juncos, R., Donato, M., Guevara, S.R., Rizzo, A., 2020. Spatiotemporal structuring factors in the Chironomidae larvae (Insecta: Diptera) assemblages of an ultraoligotrophic lake from northern Patagonia Andean range: implications for paleolimnological interpretations. *Hydrobiologia* 847, 267–291. <https://doi.org/10.1007/s10750-019-04089-w>.
- Winnell, M.H., White, D.S., 1986. The distribution of *Heterotrissocladius oliveri* saether (Diptera: Chironomidae) in Lake Michigan. *Hydrobiologia* 131, 205–214. <https://doi.org/10.1007/BF00008856>.
- Wood, S.N., 2017. *Generalized Additive Models: an Introduction with R*, second ed. Chapman and Hall/CRC. R package version 1.8-42. Available at: <https://CRAN.R-project.org/package=mgcv>.
- Woodward, C.A., Shulmeister, J., 2006. New Zealand chironomids as proxies for human-induced and natural environmental change: transfer functions for temperature and lake production (chlorophyll a). *J. Paleolimnol.* 36, 407–429. <https://doi.org/10.1007/s10933-006-9009-6>.
- Wu, J., Porinchu, D.F., Horn, S.P., Haberyan, K.A., 2015. The modern distribution of chironomid sub-fossils (Insecta: Diptera) in Costa Rica and the development of a regional chironomid-based temperature inference model. *Hydrobiologia* 742, 107–127. <https://doi.org/10.1007/s10750-014-1970-x>.
- Wu, X., de Vernal, A., Fréchet, B., Moros, M., Perner, K., 2021. The signal of climate changes over the last two millennia in the Gulf of St. Lawrence, eastern Canada. *Quaternary Research* 1–16. <https://doi.org/10.1017/qua.2021.56>.